Figure 8.1
a. Closed-loop system; **b.** equivalent transfer function

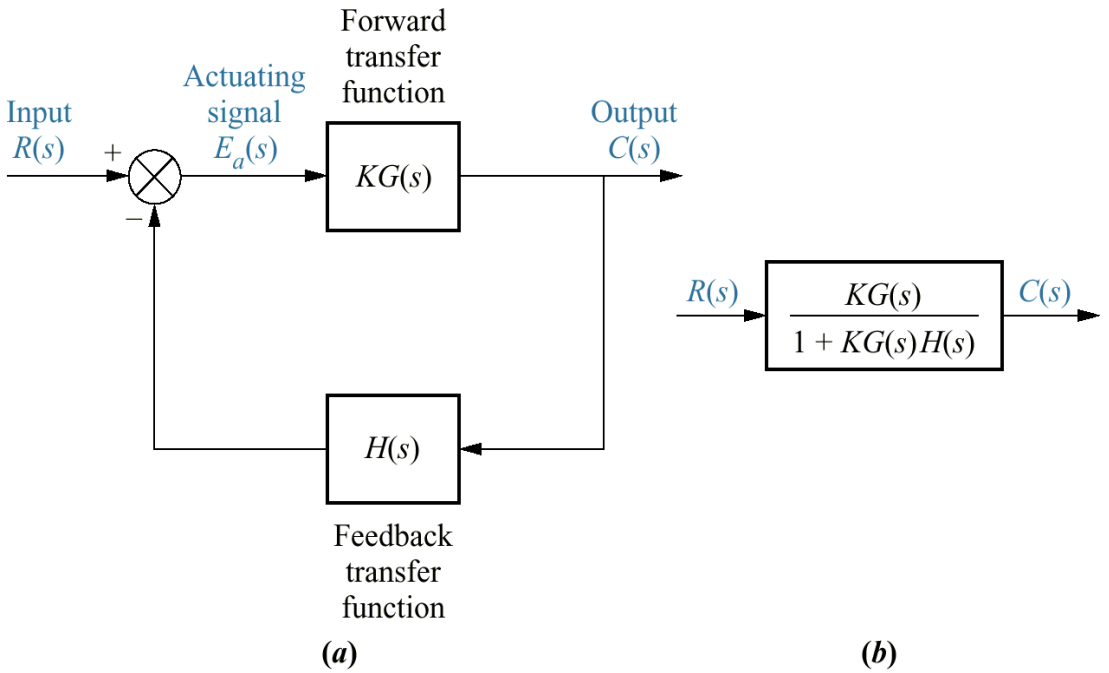

Figure 8.2
Vector representation of complex numbers:
a. s = $\sigma + j\omega$;
b. $(s + a)$;
c. alternate representation of $(s + a)$;
d. $(s + 7)|_{s \to 5 + j2}$

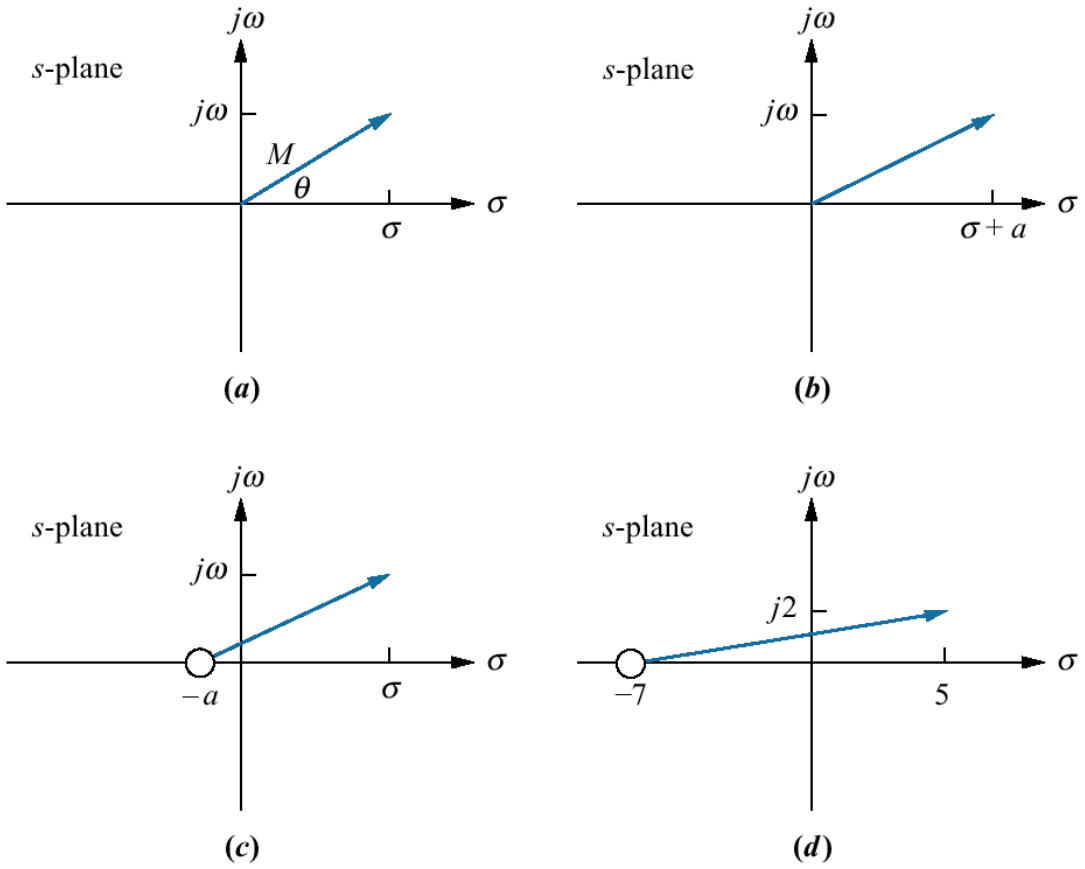

Figure 8.3
Vector representation of Eq. (8.7)

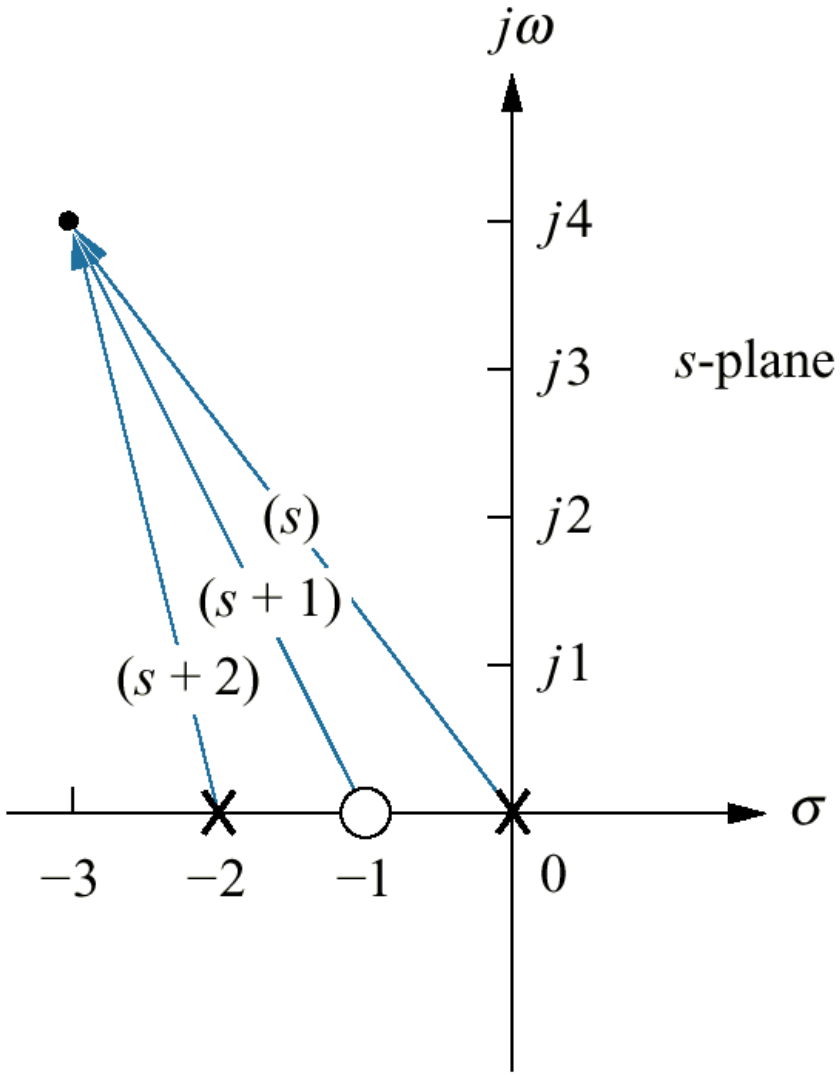

Figure 8.4

a. CameraMan® Presenter Camera System automatically follows a subject who wears infrared sensors on their front and back (the front sensor is also a microphone); tracking commands and audio are relayed to CameraMan via a radio frequency link from a unit worn by the subject.
b. block diagram.
c. closed-loop transfer function.

Courtesy of ParkerVision.

(*a*)

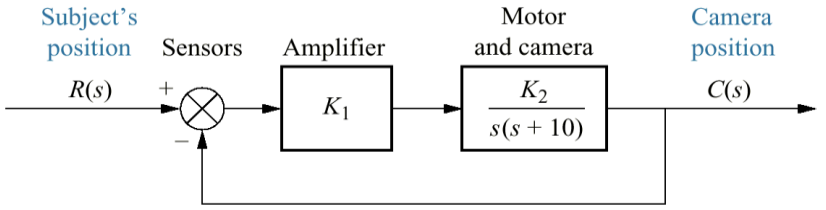

(*b*)

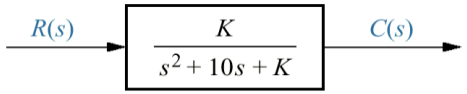

where $K = K_1K_2$

(*c*)

Table 8.1
Pole location as a function of gain for the system of Figure 8.4

K	Pole 1	Pole 2
0	-10	0
5	-9.47	-0.53
10	-8.87	-1.13
15	-8.16	-1.84
20	-7.24	-2.76
25	-5	-5
30	$-5 + j2.24$	$-5 - j2.24$
35	$-5 + j3.16$	$-5 - j3.16$
40	$-5 + j3.87$	$-5 - j3.87$
45	$-5 + j4.47$	$-5 - j4.47$
50	$-5 + j5$	$-5 - j5$

Figure 8.5
a. Pole plot from Table 8.1;
b. root locus

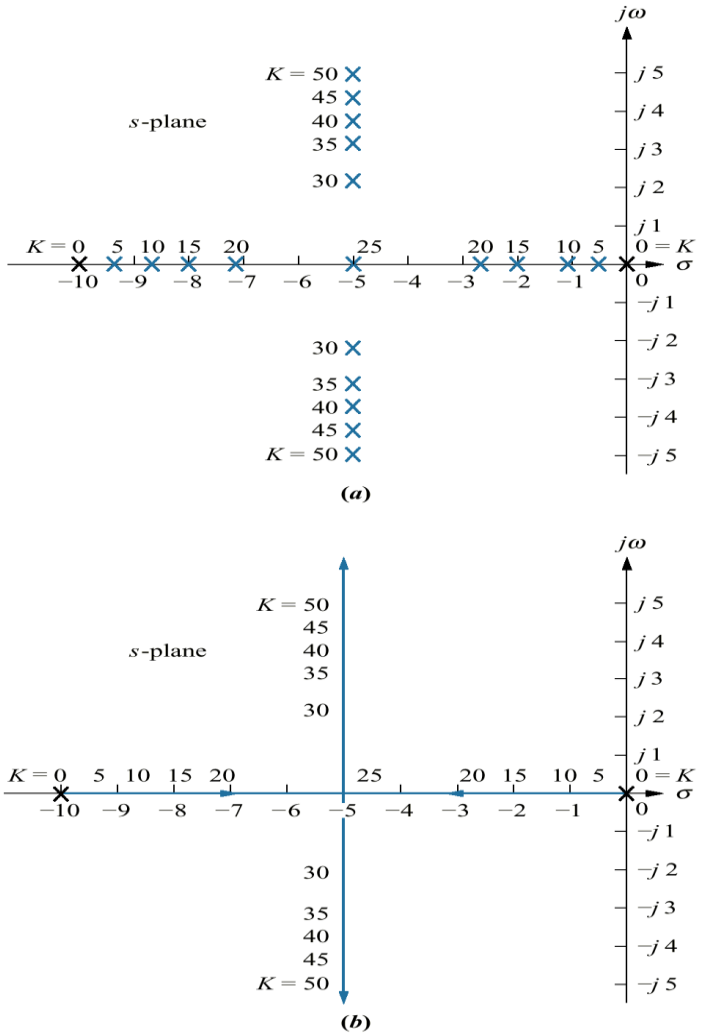

Figure 8.6
a. Example system;
b. pole-zero plot of G (s)

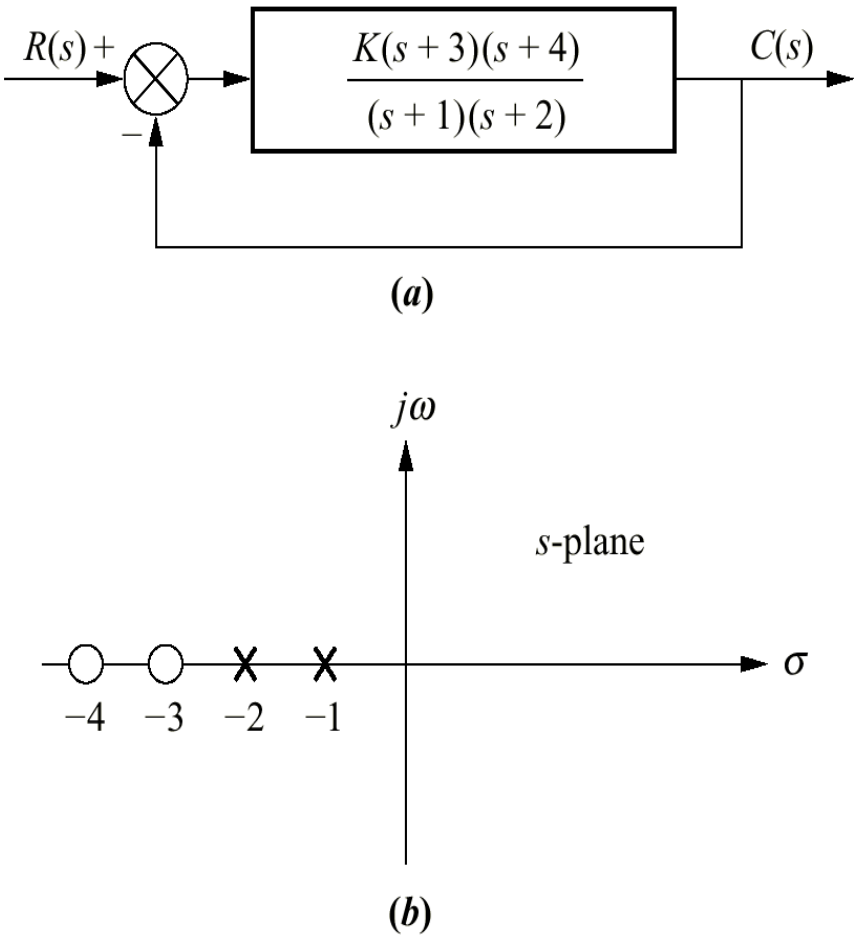

Figure 8.7
Vector representation of *G*(s) from Figure 8.6(a) at -2+ *j* 3

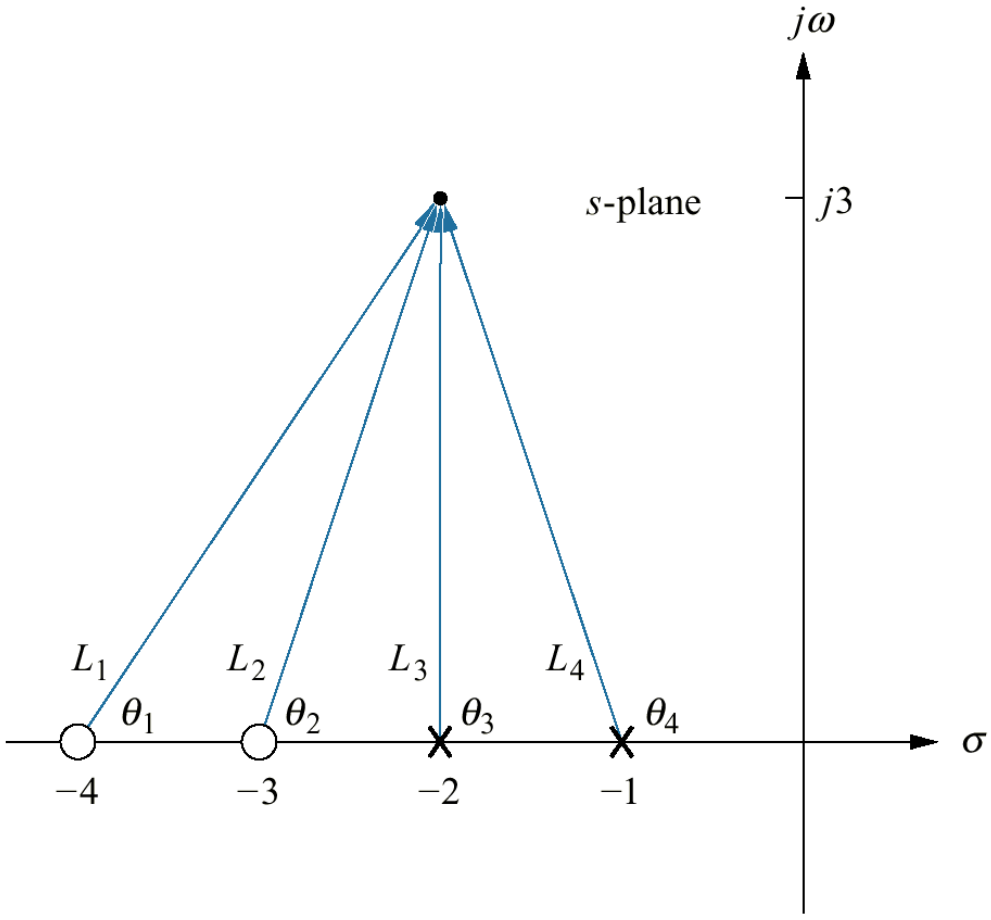

Figure 8.8
Poles and zeros of a general open-loop system with test points, P_i, on the real axis

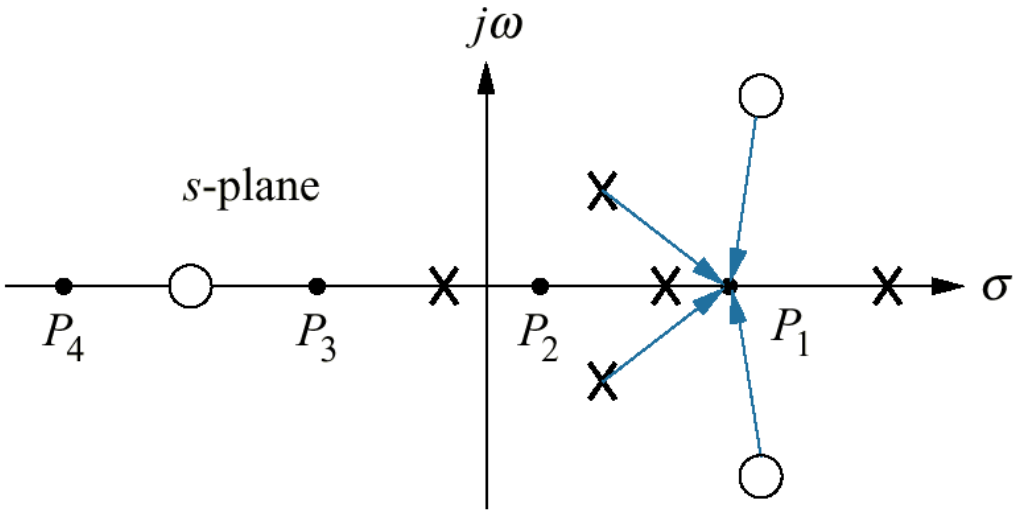

Figure 8.9
Real-axis segments of the root locus for the system of Figure 8.6

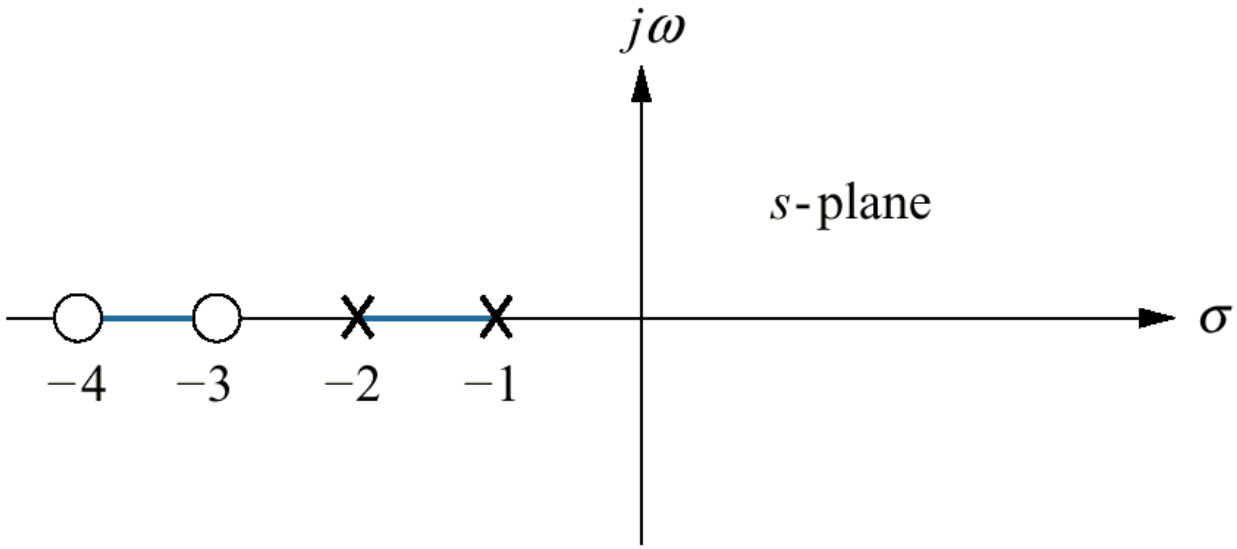

Figure 8.10
Complete root locus for the system of Figure 8.6

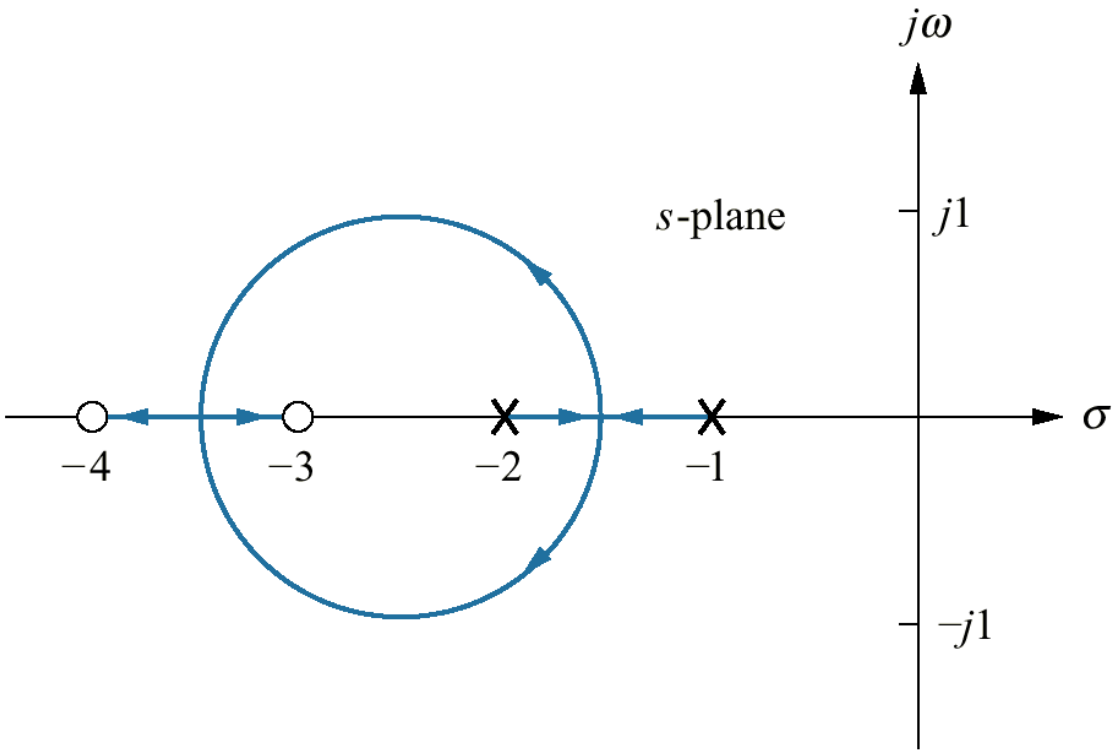

Figure 8.11
System for
Example 8.2

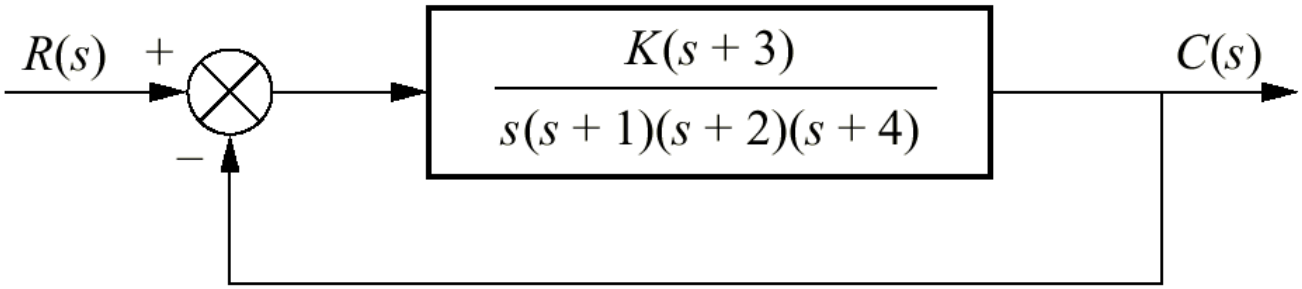

Figure 8.12
Root locus and asymptotes for the system of Figure 8.11

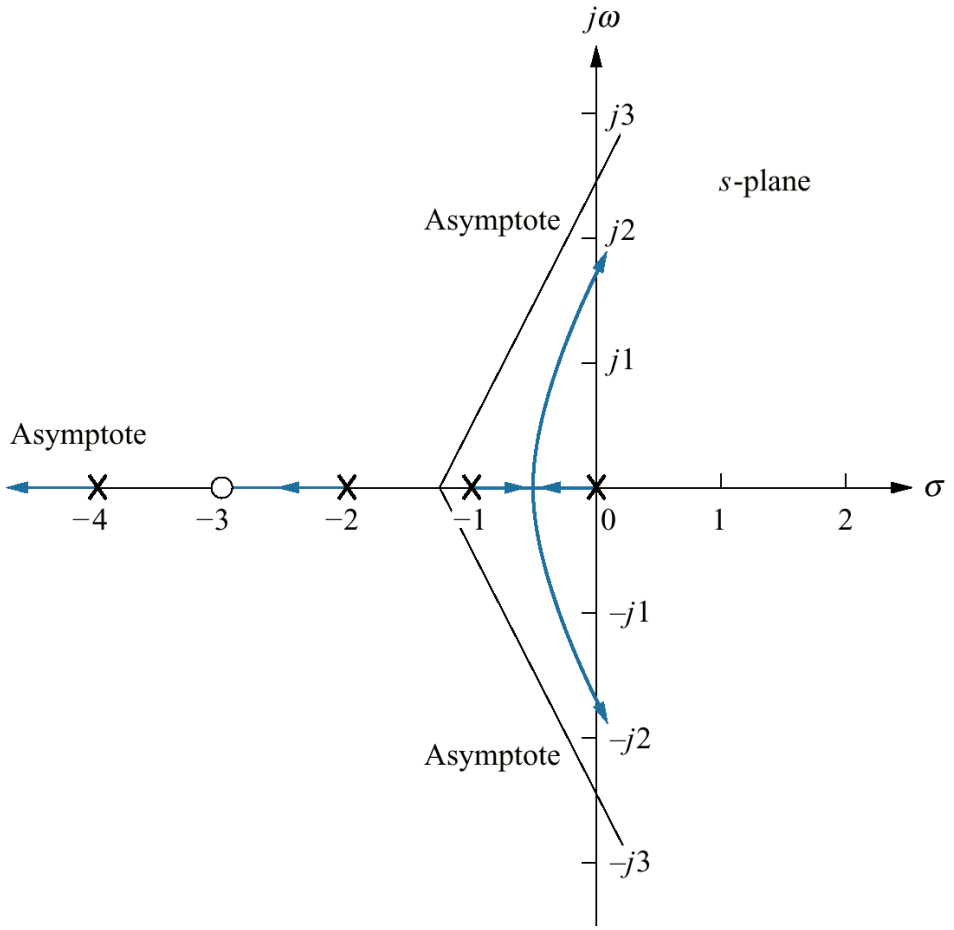

Figure 8.13
Root locus example showing real- axis breakaway ($-\sigma_1$) and break-in points (σ_2)

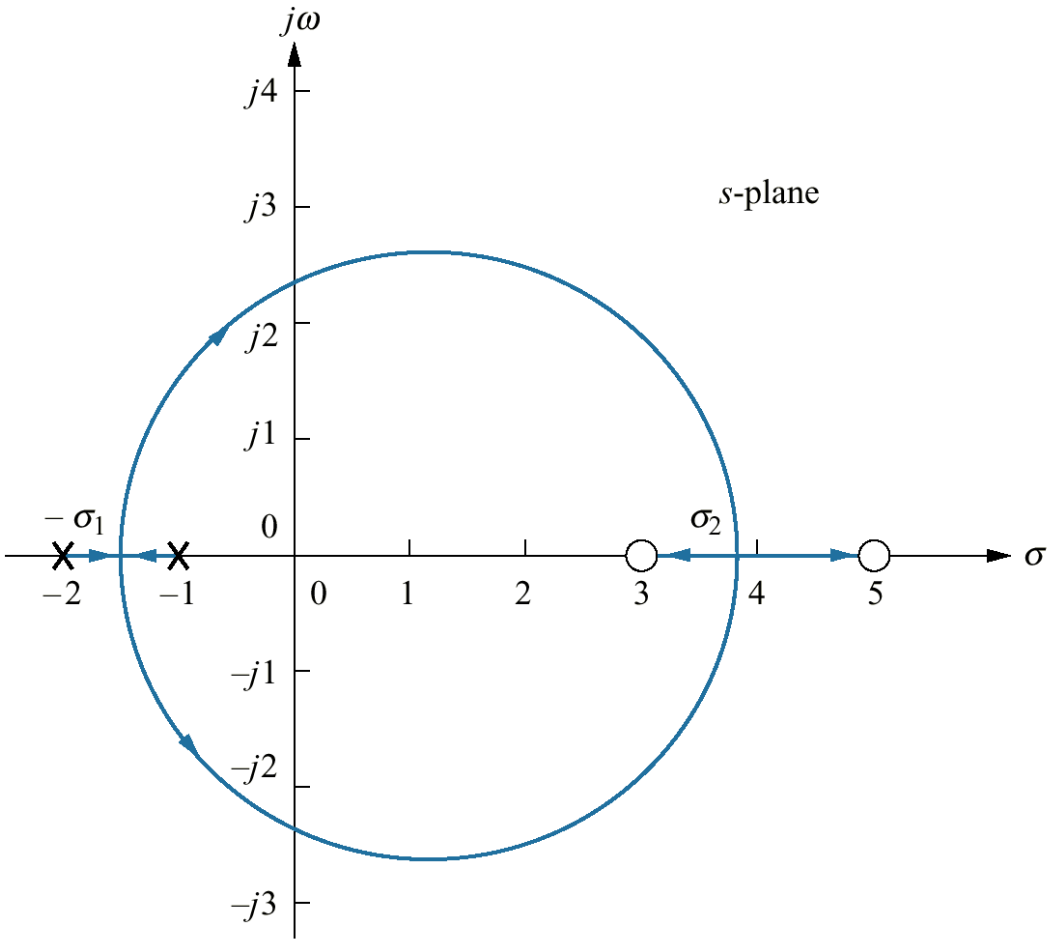

Figure 8.14
Variation of gain along the real axis for the root locus of
Figure 8.13

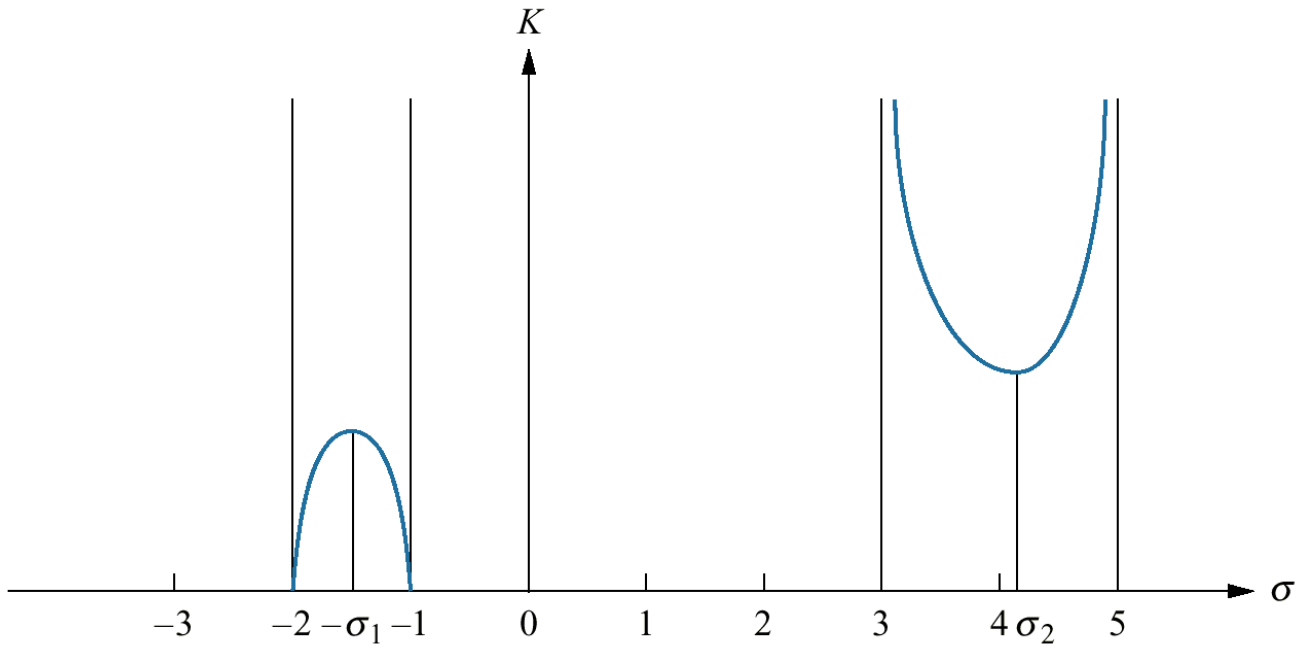

Table 8.2
Data for breakaway and break-in points for the root locus of Figure 8.13

Real axis value	Gain	
−1.41	0.008557	
−1.42	0.008585	
−1.43	0.008605	
−1.44	0.008617	
−1.45	0.008623	← Max. gain: breakaway
−1.46	0.008622	
3.3	44.686	
3.4	37.125	
3.5	33.000	
3.6	30.667	
3.7	29.440	
3.8	29.000	← Min. gain: break-in
3.9	29.202	

s^4	1	14	$3K$
s^3	7	$8 + K$	
s^2	$90 - K$	$21K$	
s^1	$\dfrac{-K^2 - 65K + 720}{90 - K}$		
s^0	$21K$		

Table 8.3
Routh table for Eq. (8.40)

Figure 8.15
Open-loop poles and zeros and calculation of:
a. angle of departure;
b. angle of arrival

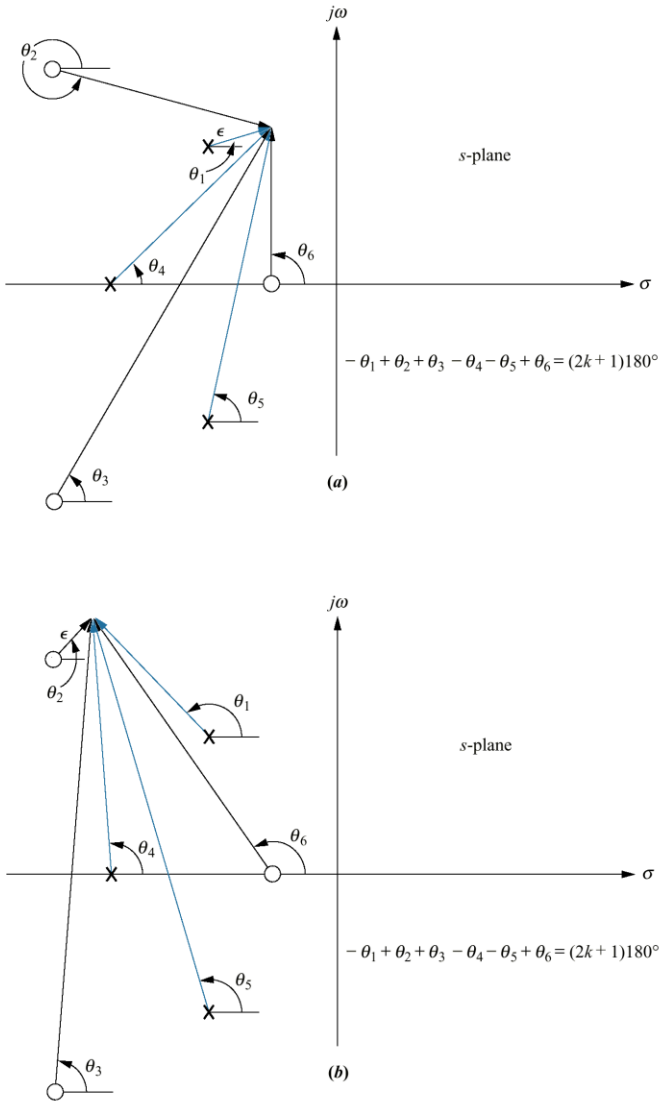

Figure 8.16
Unity feedback system
with complex poles

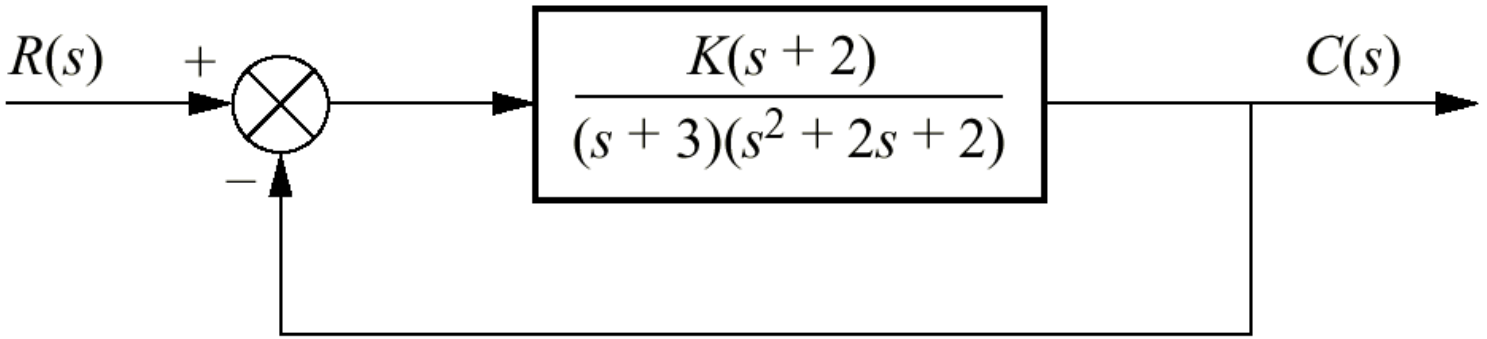

Figure 8.17
Root locus for system of Figure 8.16 showing angle of departure

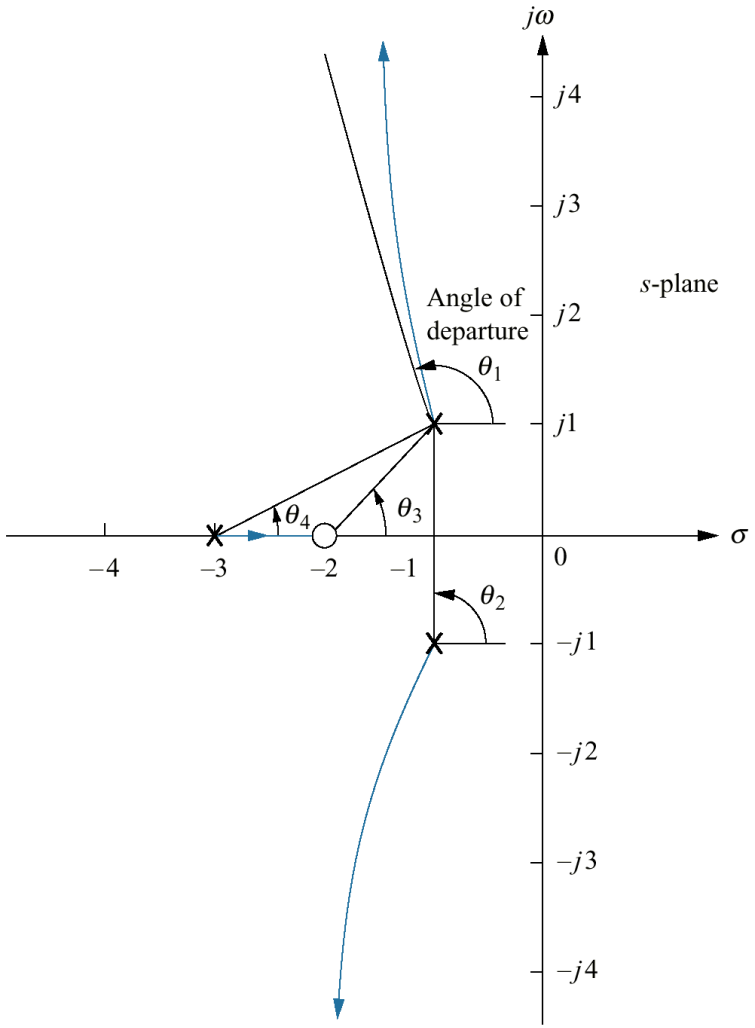

Figure 8.18
Finding and calibrating exact points on the root locus of
Figure 8.12

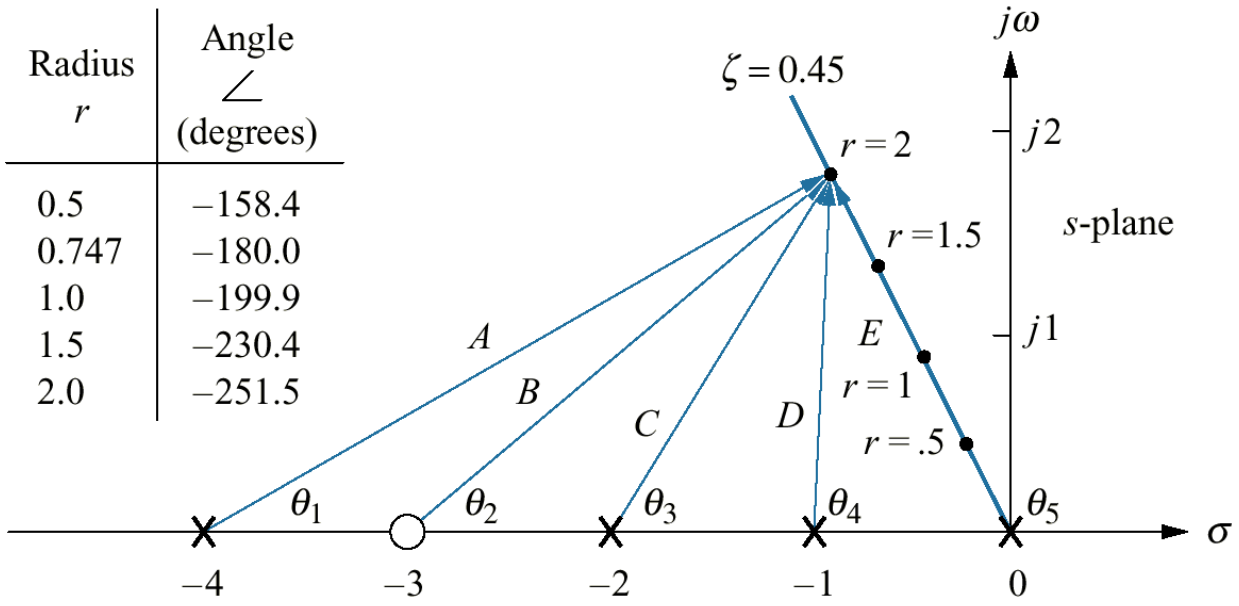

Figure 8.19
a. System for Example 8.7;
b. root locus sketch

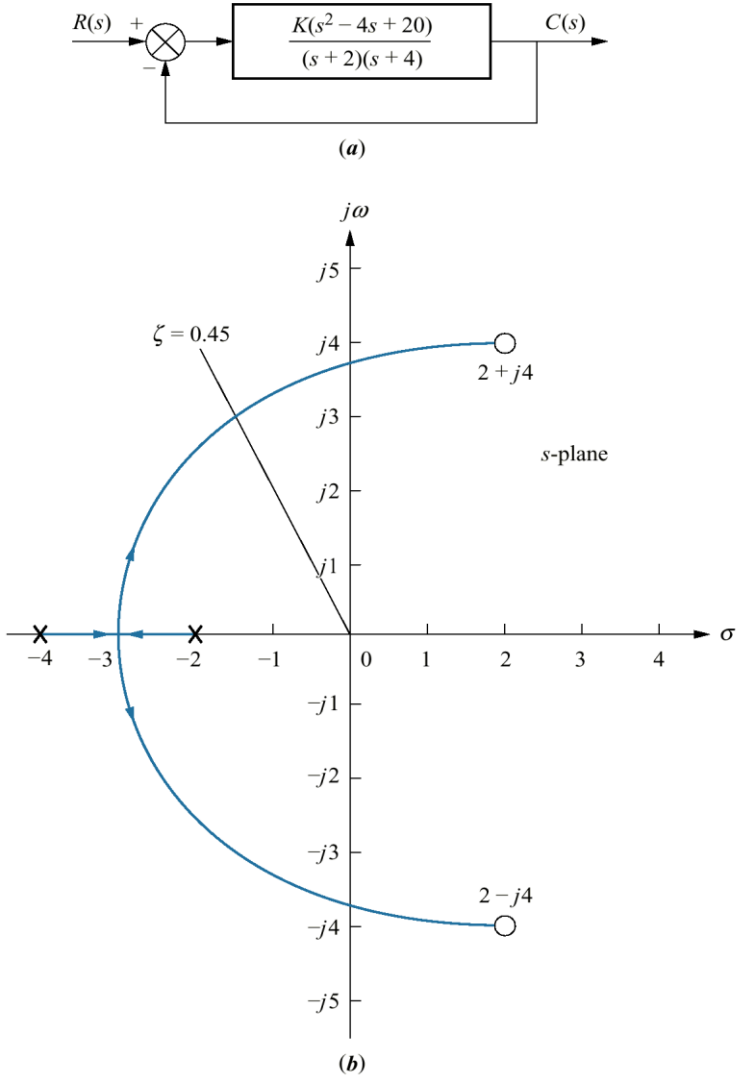

Figure 8.20
Making second-order approximations

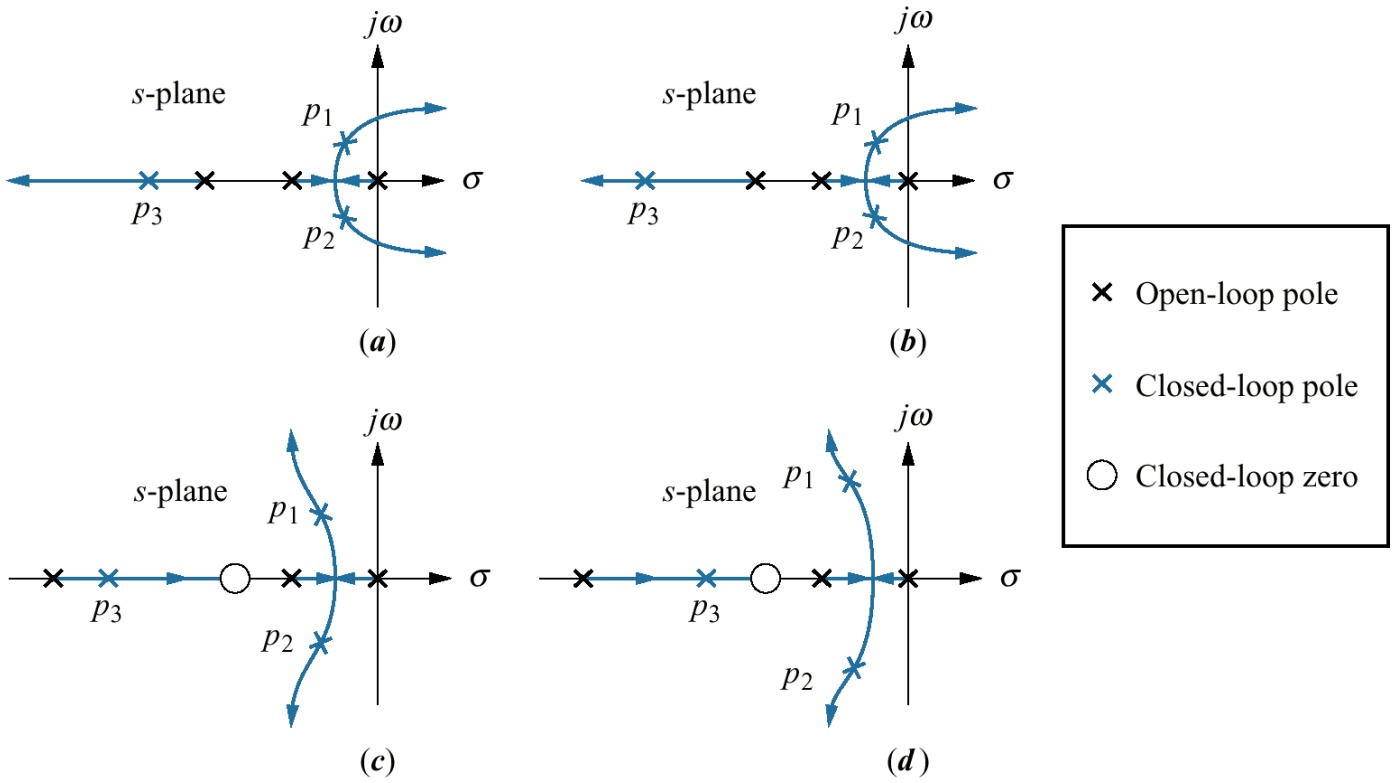

Figure 8.21
System for
Example 8.8

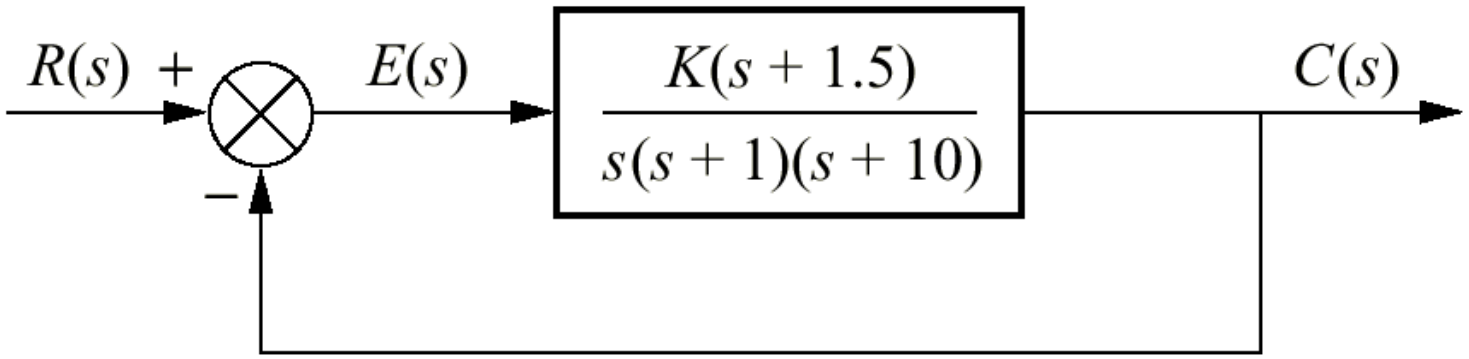

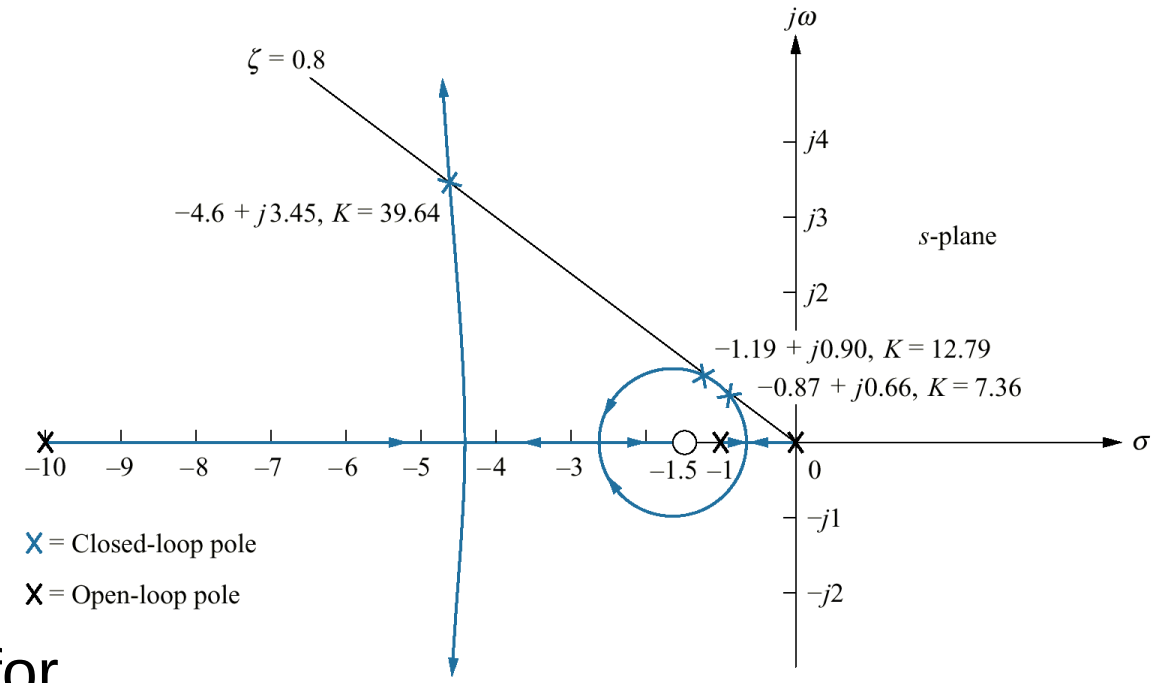

Figure 8.22 Root locus for Example 8.8

Table 8.4
Characteristics of the system of Example 8.8

Case	Closed-loop poles	Closed-loop zero	Gain	Third closed-loop pole	Settling time	Peak time	K_v
1	$-0.87 \pm j0.66$	$-1.5 + j0$	7.36	-9.25	4.60	4.76	1.1
2	$-1.19 \pm j0.90$	$-1.5 + j0$	12.79	-8.61	3.36	3.49	1.9
3	$-4.60 \pm j3.45$	$-1.5 + j0$	39.64	-1.80	0.87	0.91	5.9

Figure 8.23
Second- and third-order responses for Example 8.8:
a. Case 2;
b. Case 3

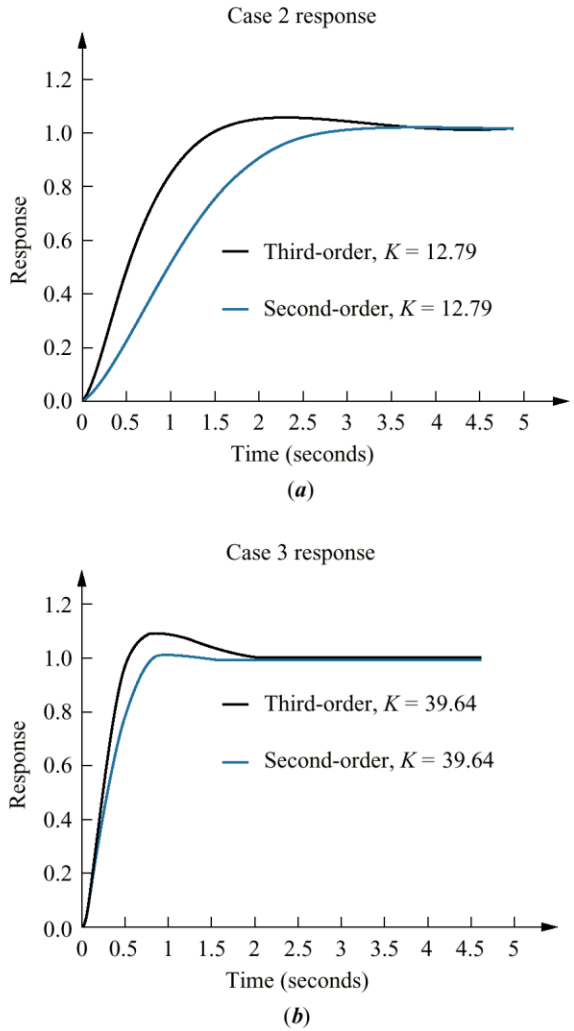

Figure 8.24
System requiring a root locus calibrated with p_1 as a parameter

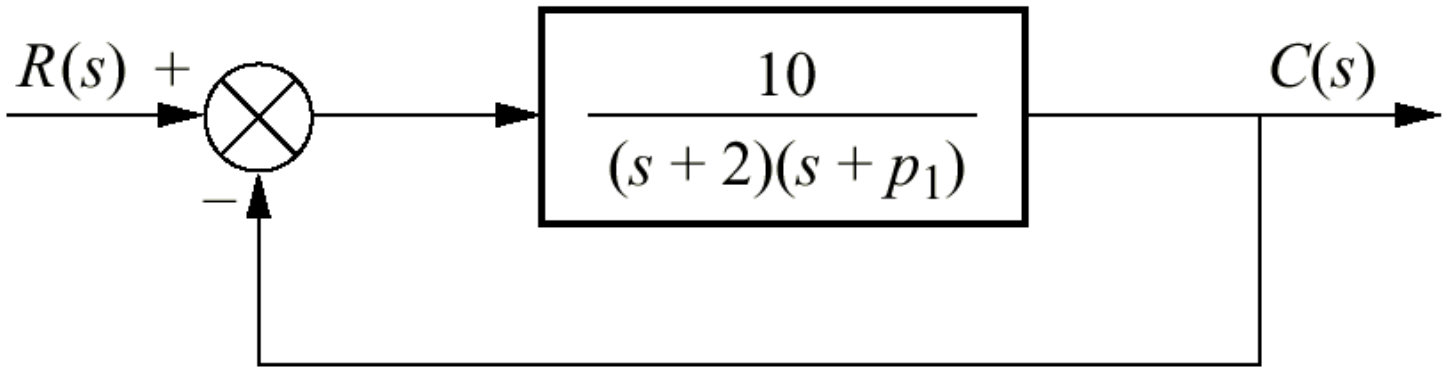

Figure 8.25
Root locus for the system of Figure 8.24, with p_1 as a parameter

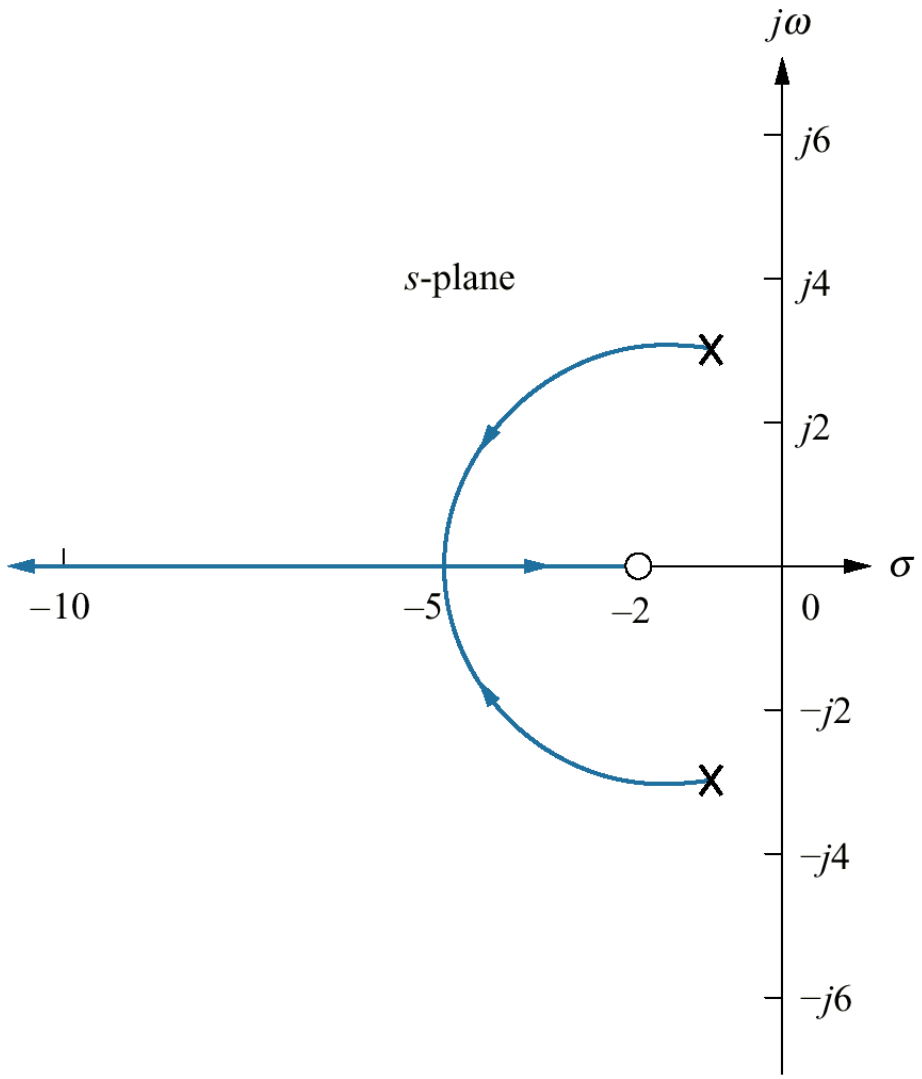

Figure 8.26
Positive-feedback system

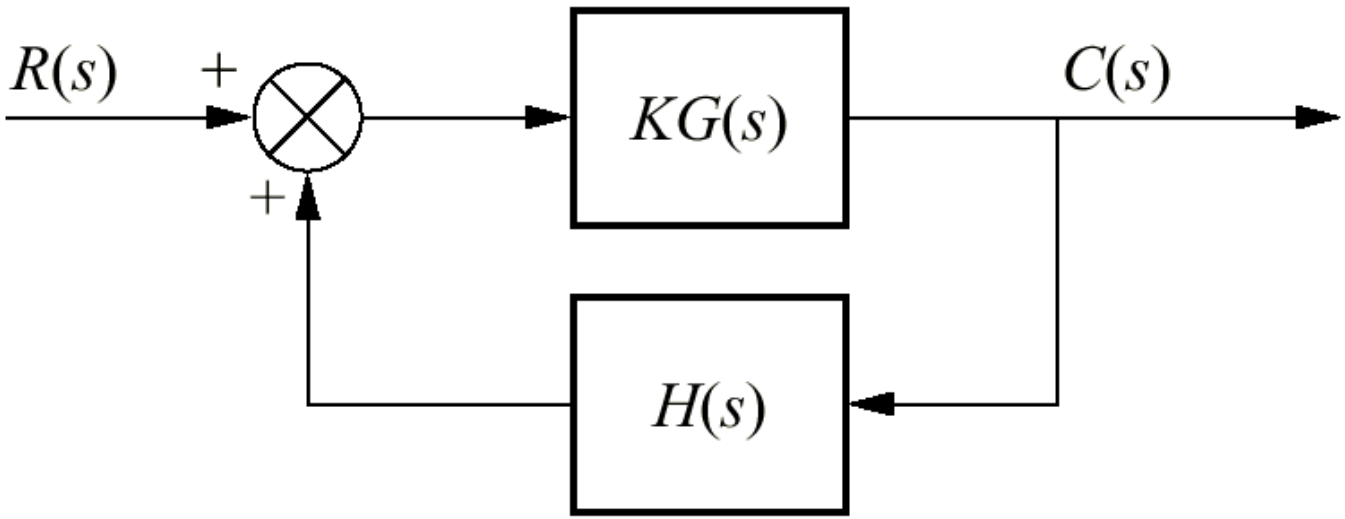

Figure 8.27
a. Equivalent positive-feedback system for Example 8.9;
b. root locus

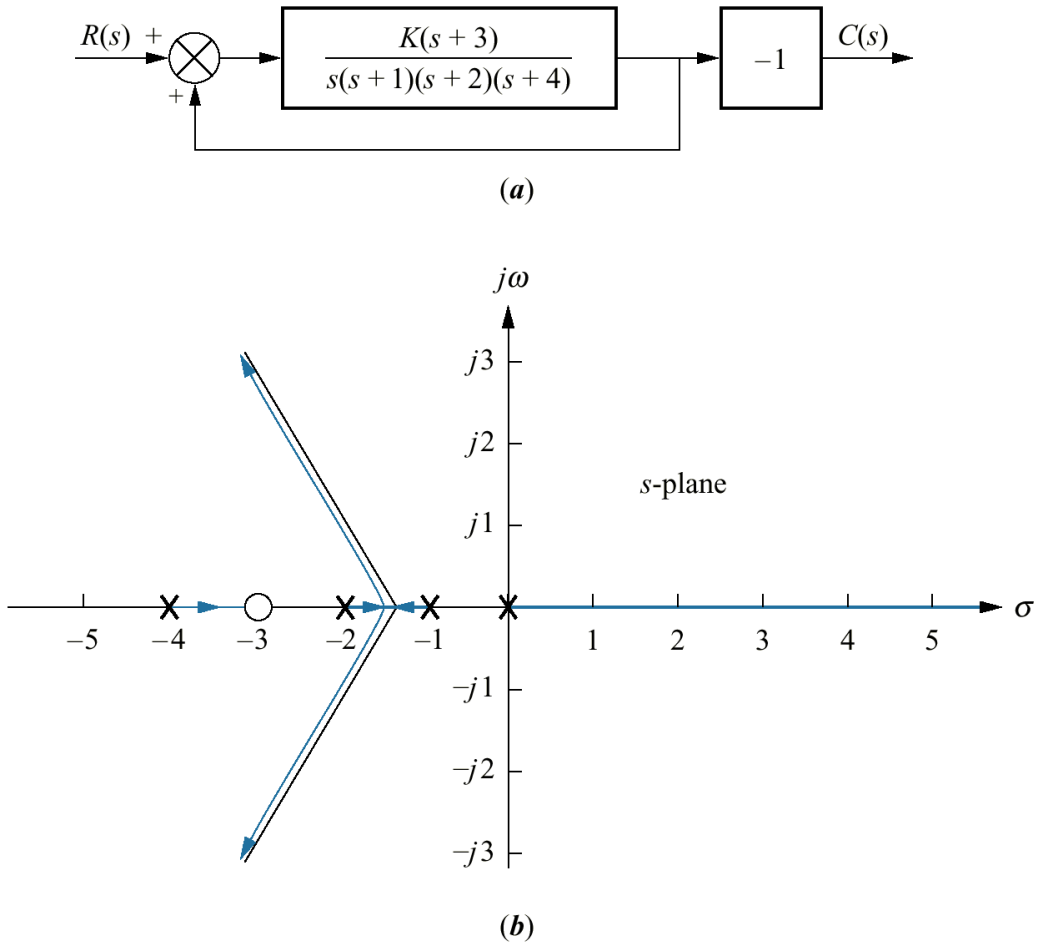

Figure 8.28
Portion of the root locus for the antenna control system

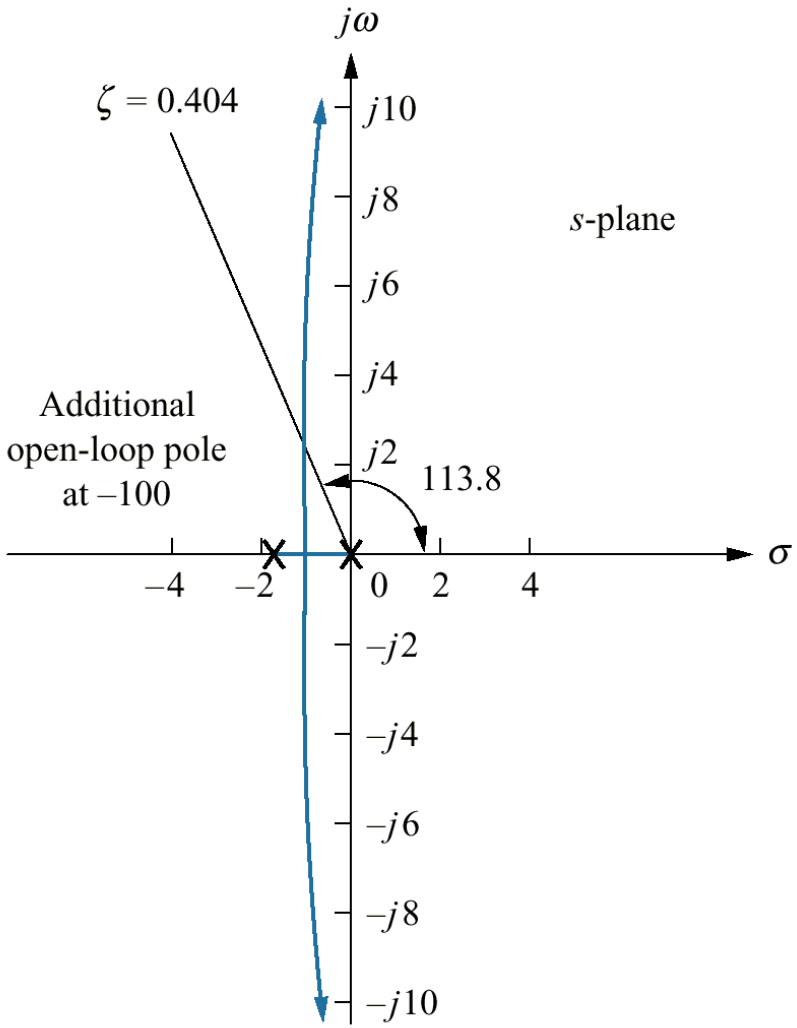

Figure 8.29
Step response of the gain-adjusted antenna control system

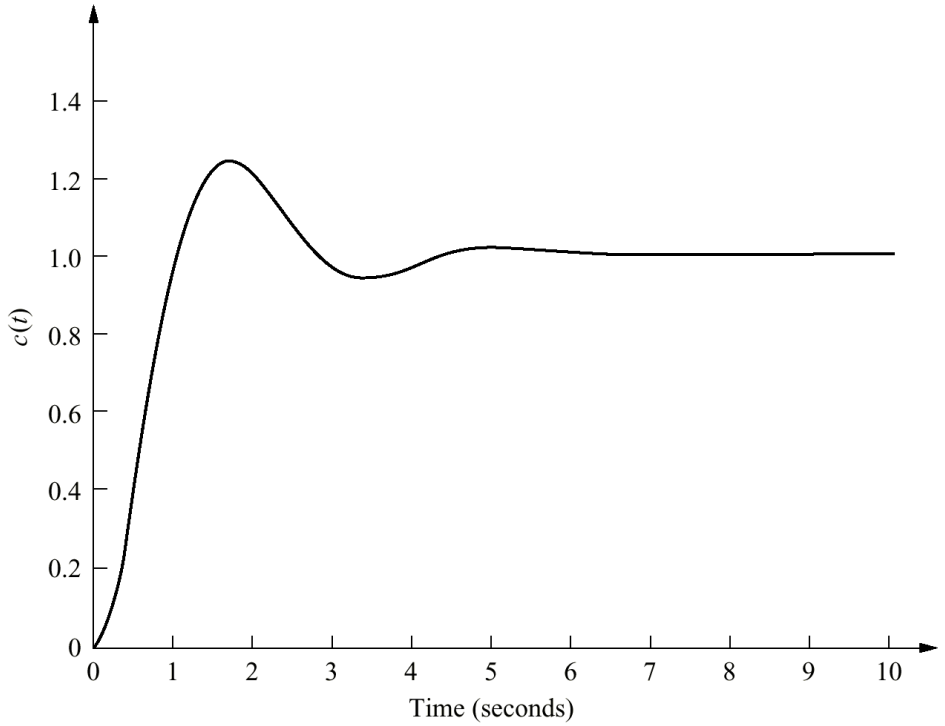

Figure 8.30
Root locus of pitch control loop without rate feedback, UFSS vehicle

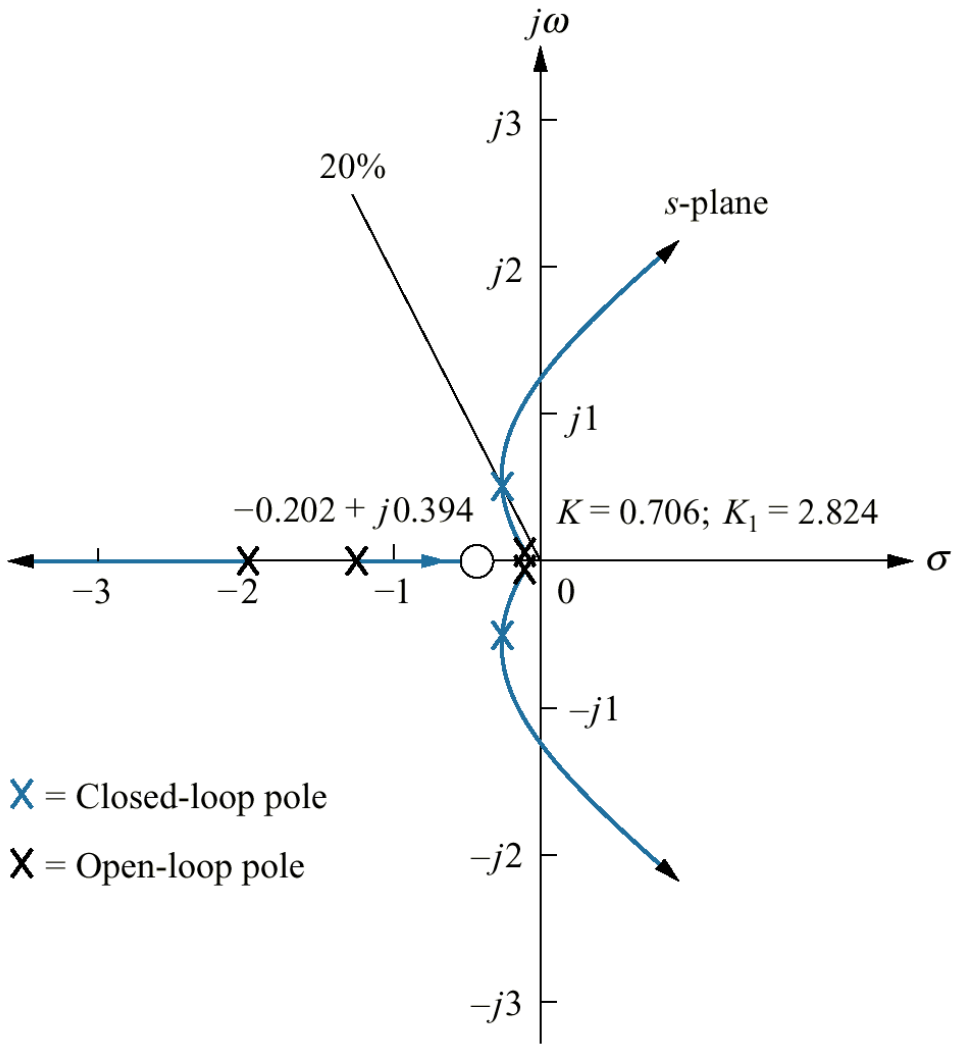

Figure 8.31 Computer simulation of step response of pitch control loop without rate feedback, UFSS vehicle

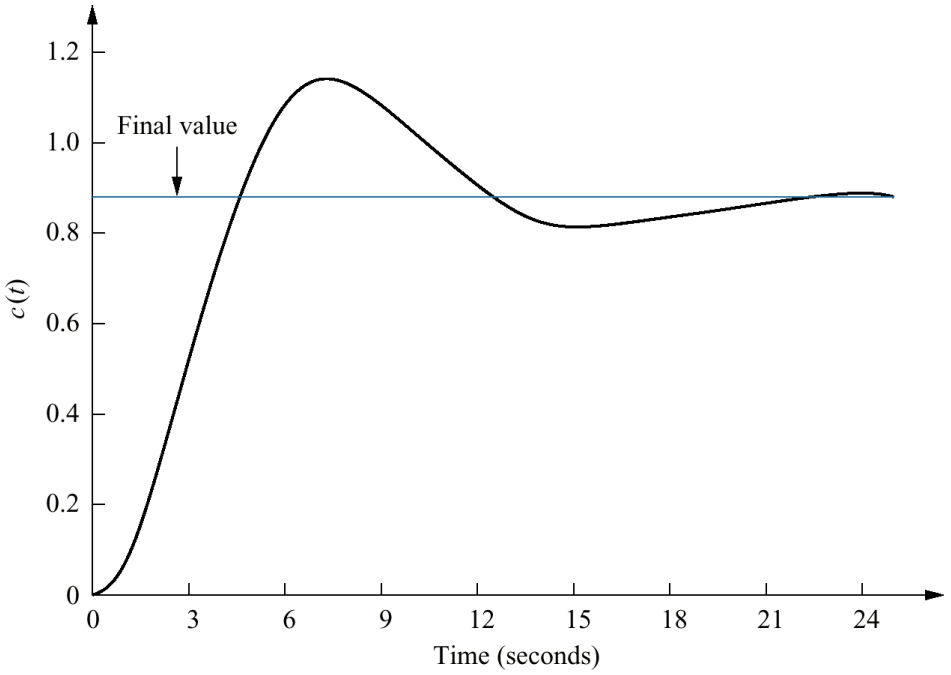

Figure 8.32
Root locus of pitch control loop with rate feedback, UFSS vehicle

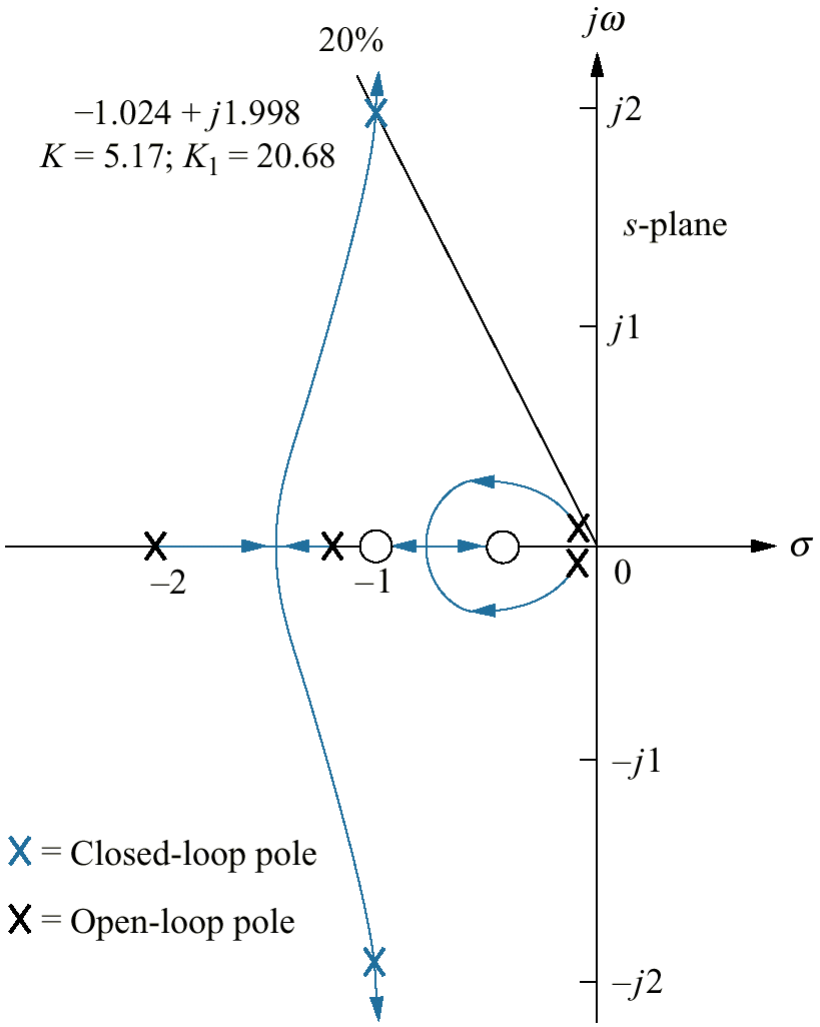

Figure 8.33
Computer simulation of step response of pitch control loop with rate feedback, UFSS vehicle

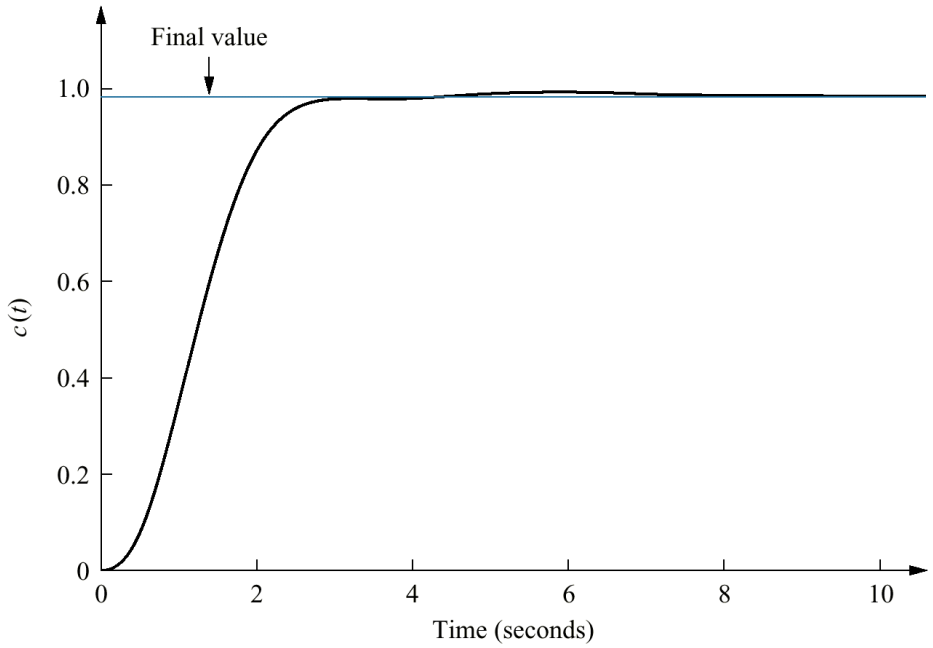

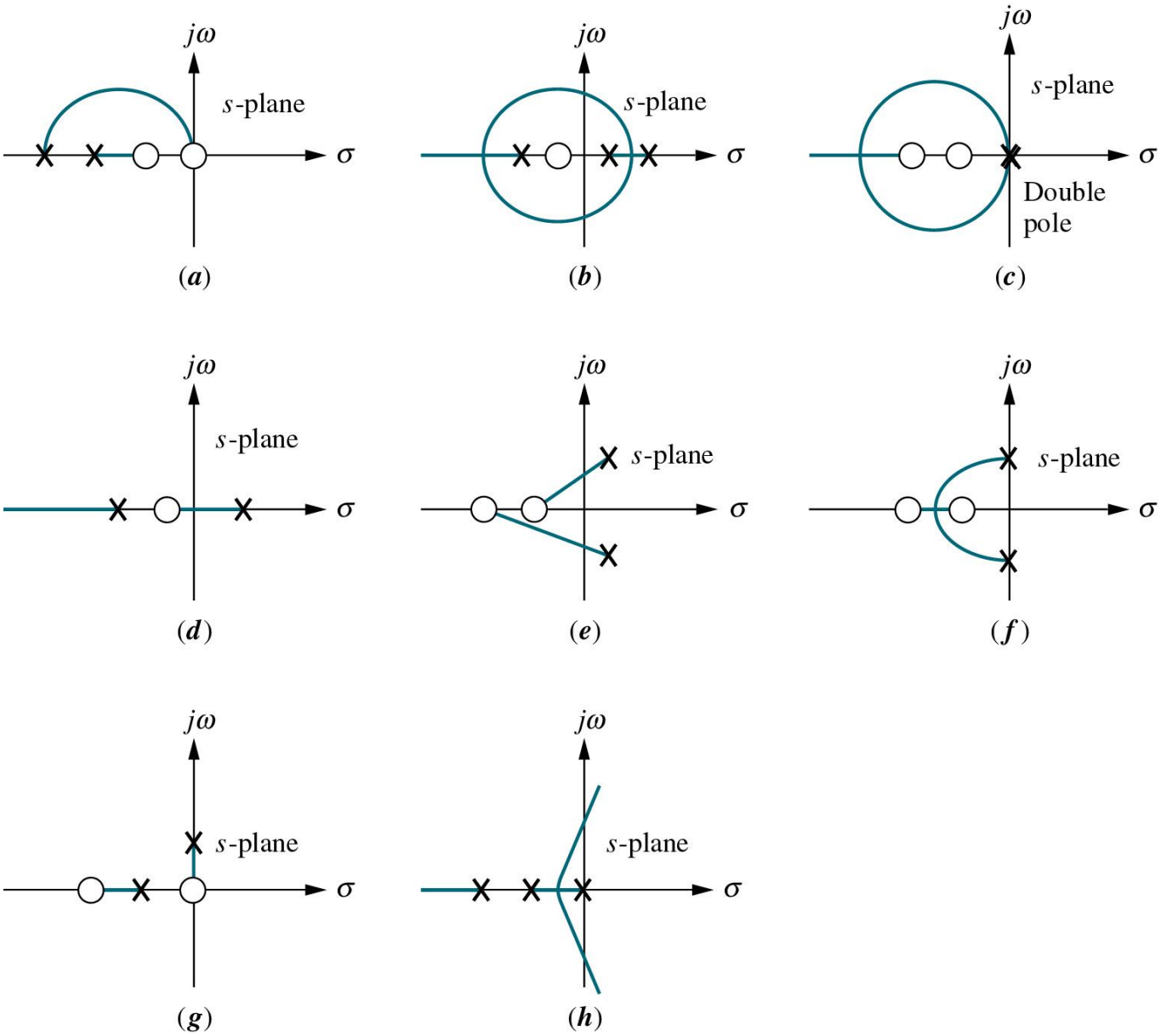

Figure P8-1 (p. 474)

Figure P8.2

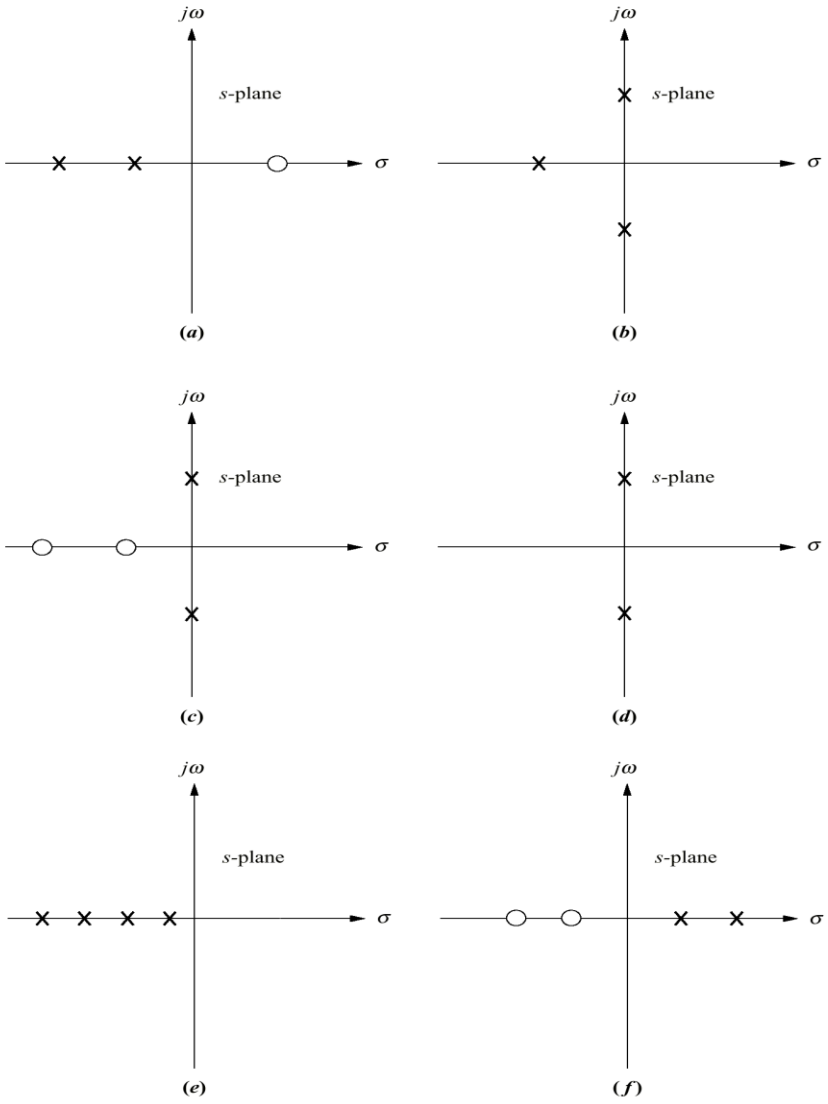
jω
s-plane
σ
(a)
jω
s-plane
σ
(b)
jω
s-plane
σ
(c)
jω
s-plane
σ
(d)
jω
s-plane
σ
(e)
jω
s-plane
σ
(f)

Figure P8.3

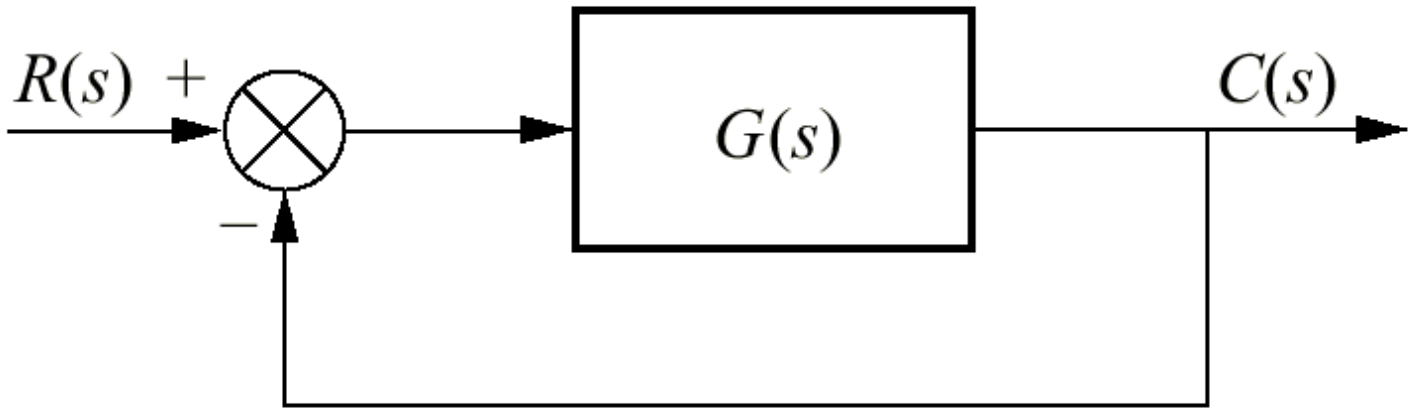

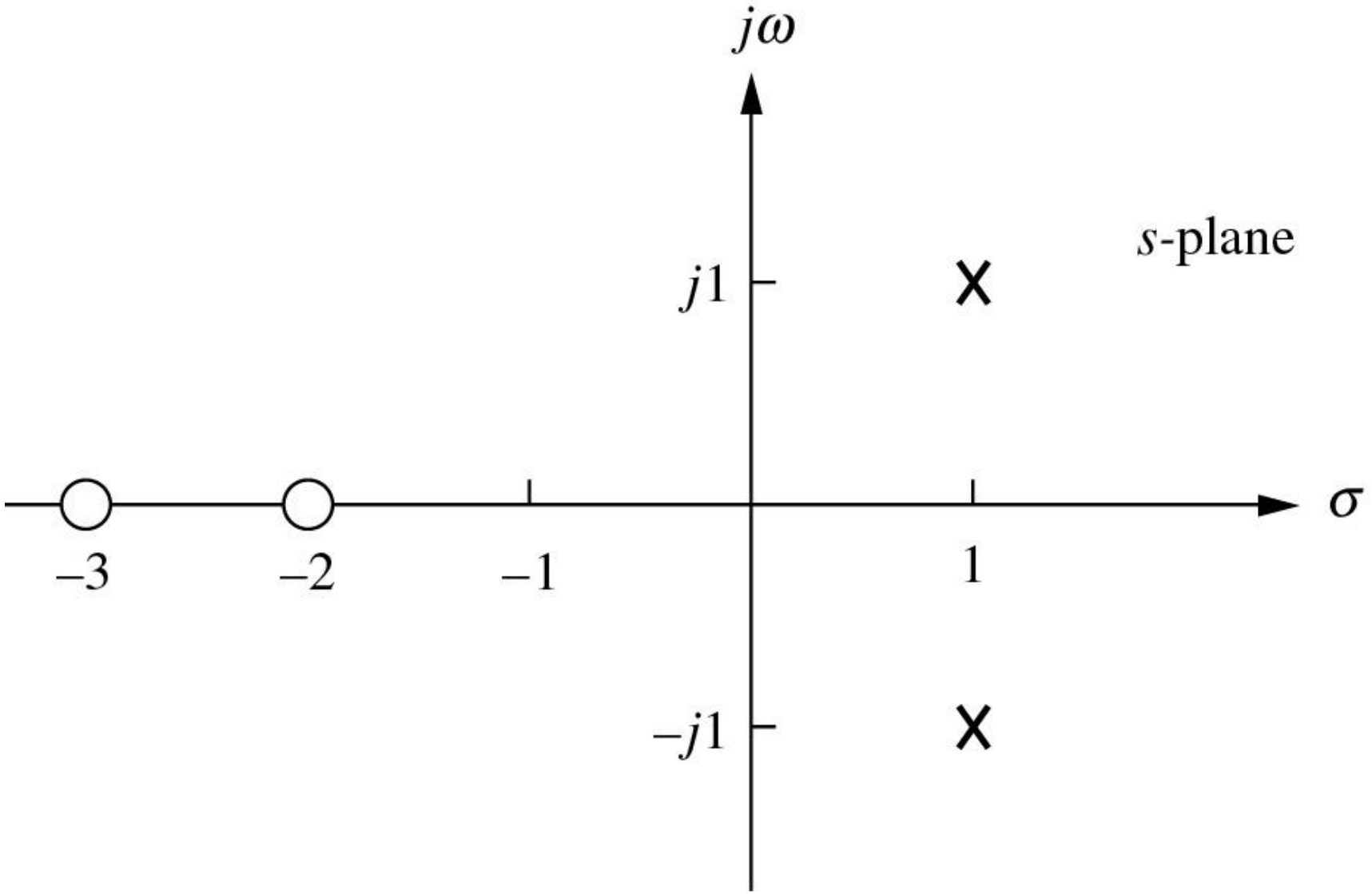

Figure P8-4 (p. 476)

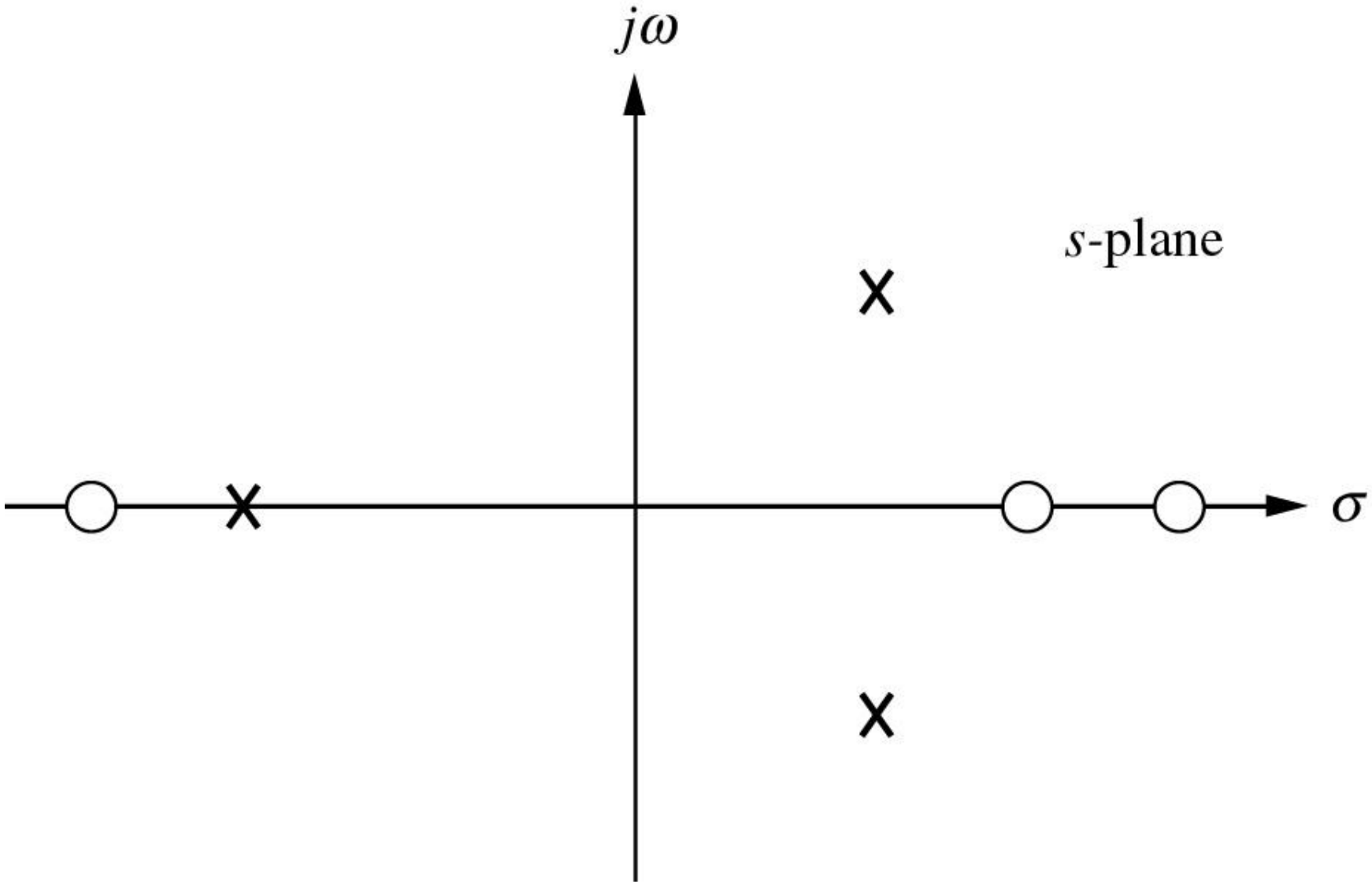

Figure P8-5 (p. 477)

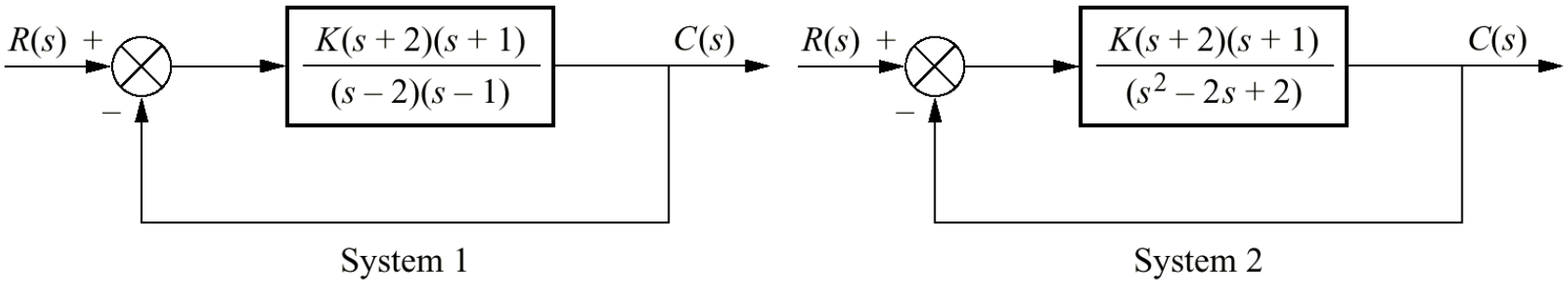

Figure P8.6

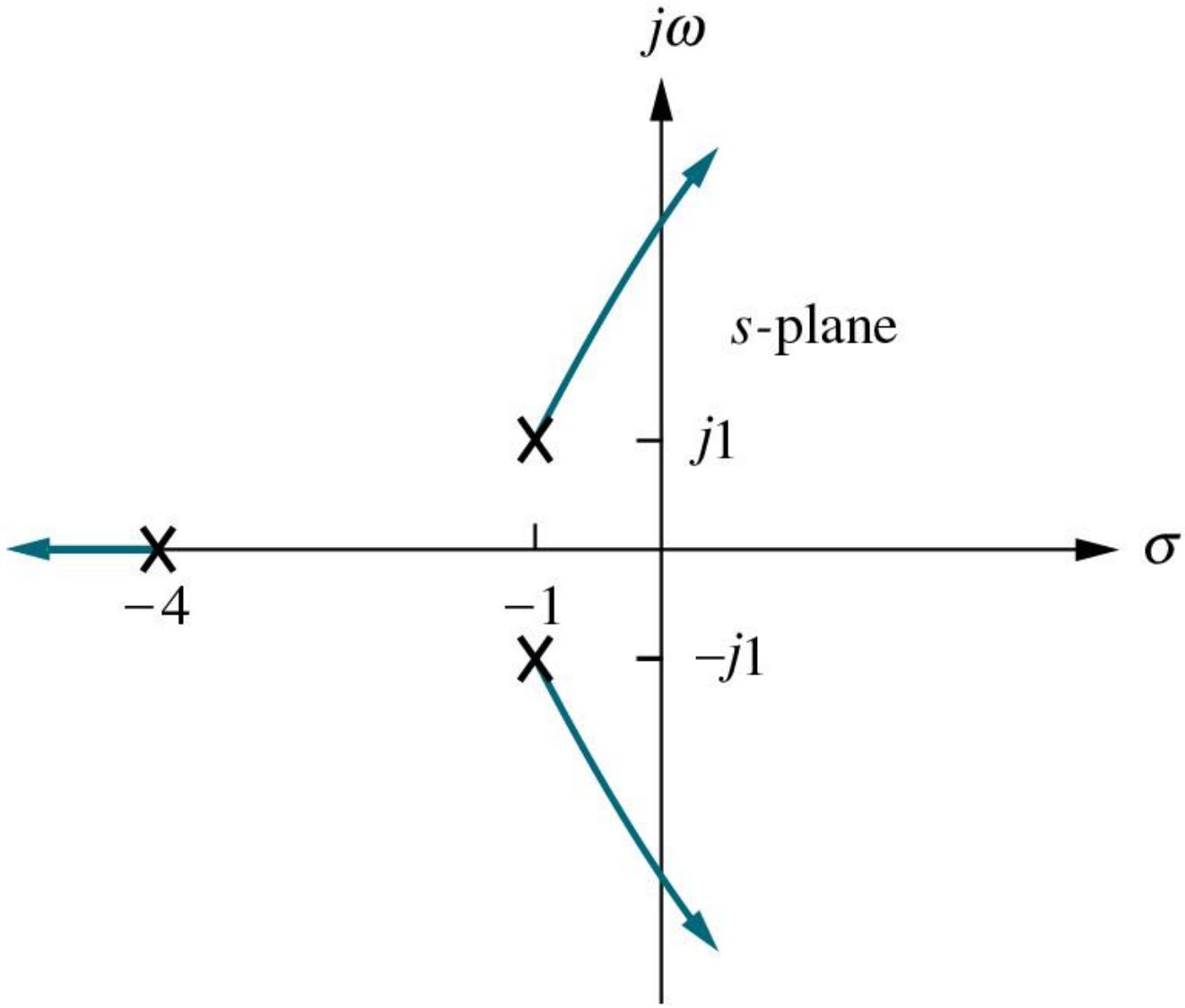

Figure P8-7 (p. 479)

Figure P8.8

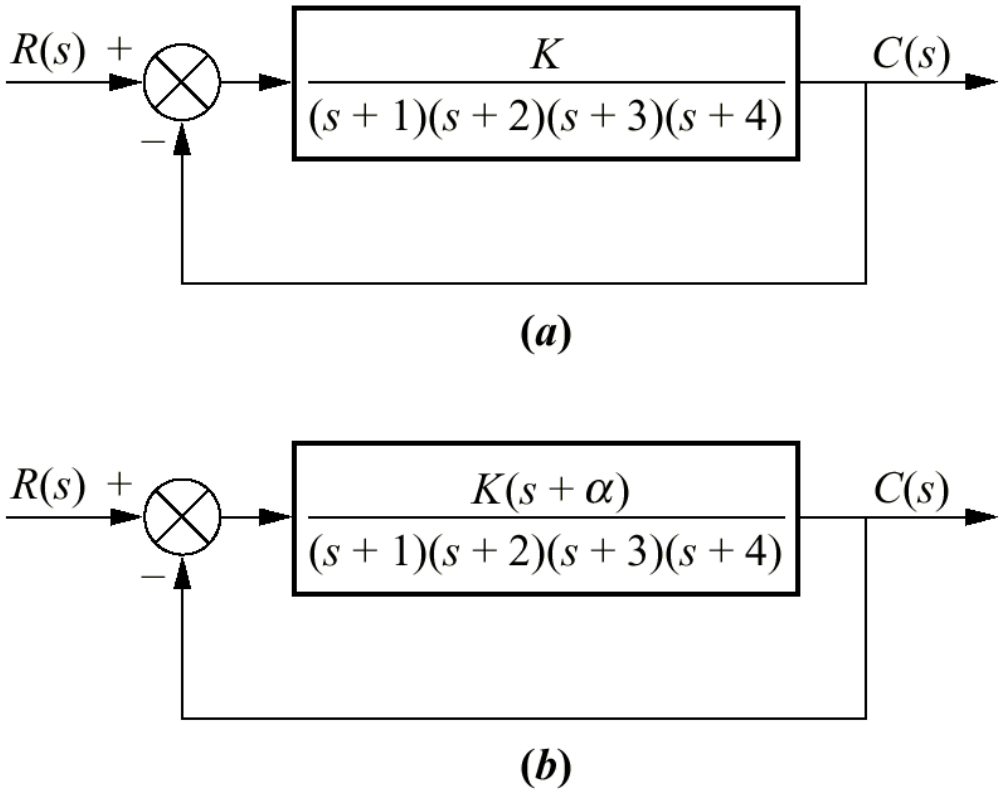

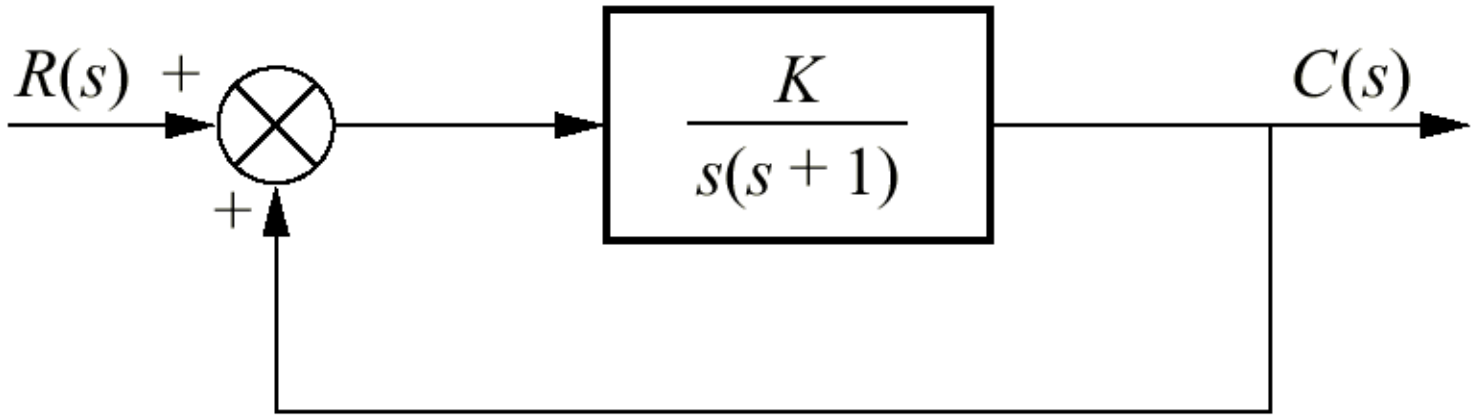

Figure P8.9

Figure P8.10

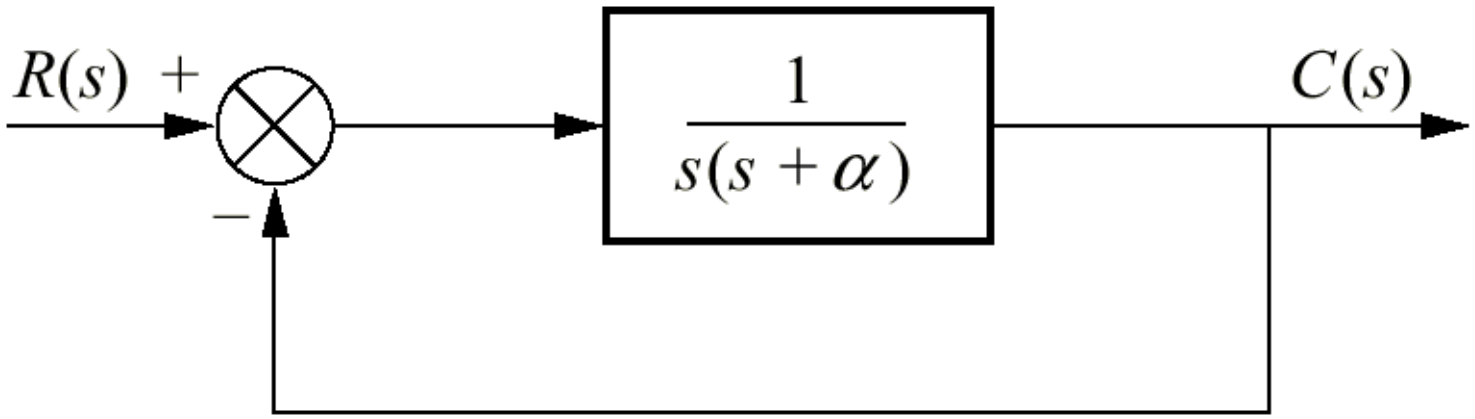

Figure P8.11

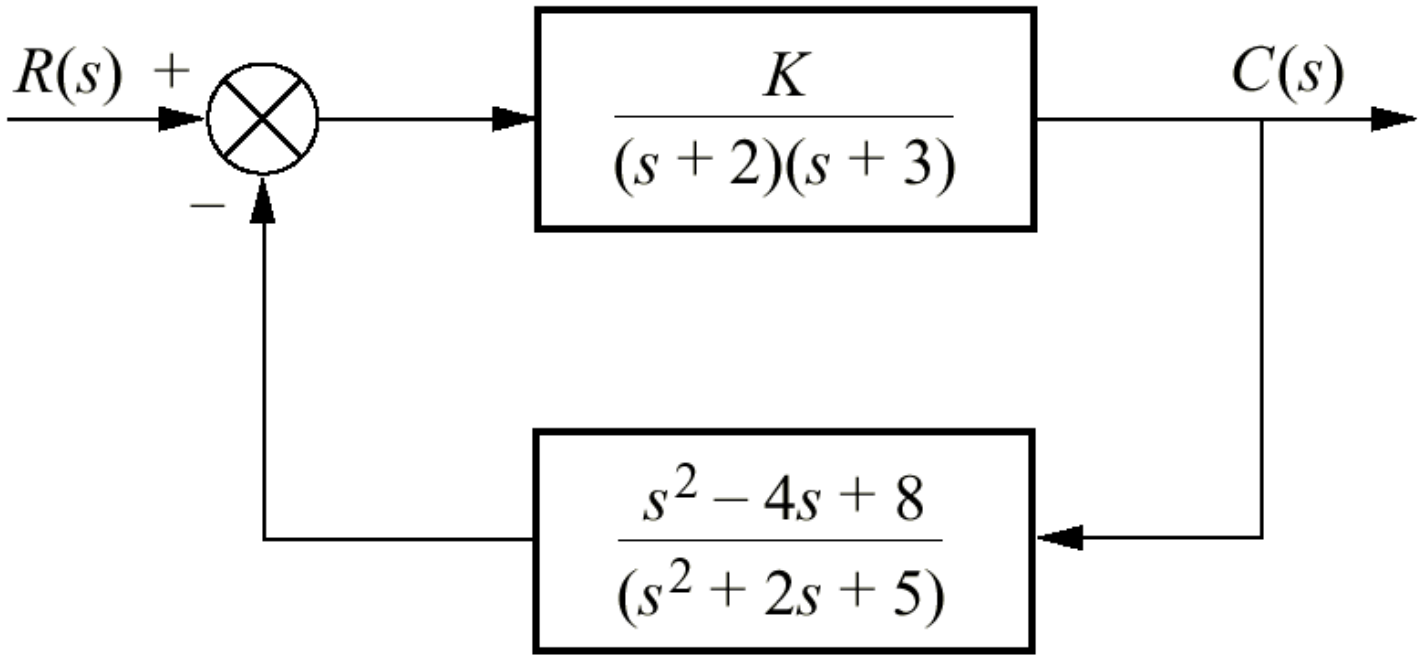

Figure P8.12

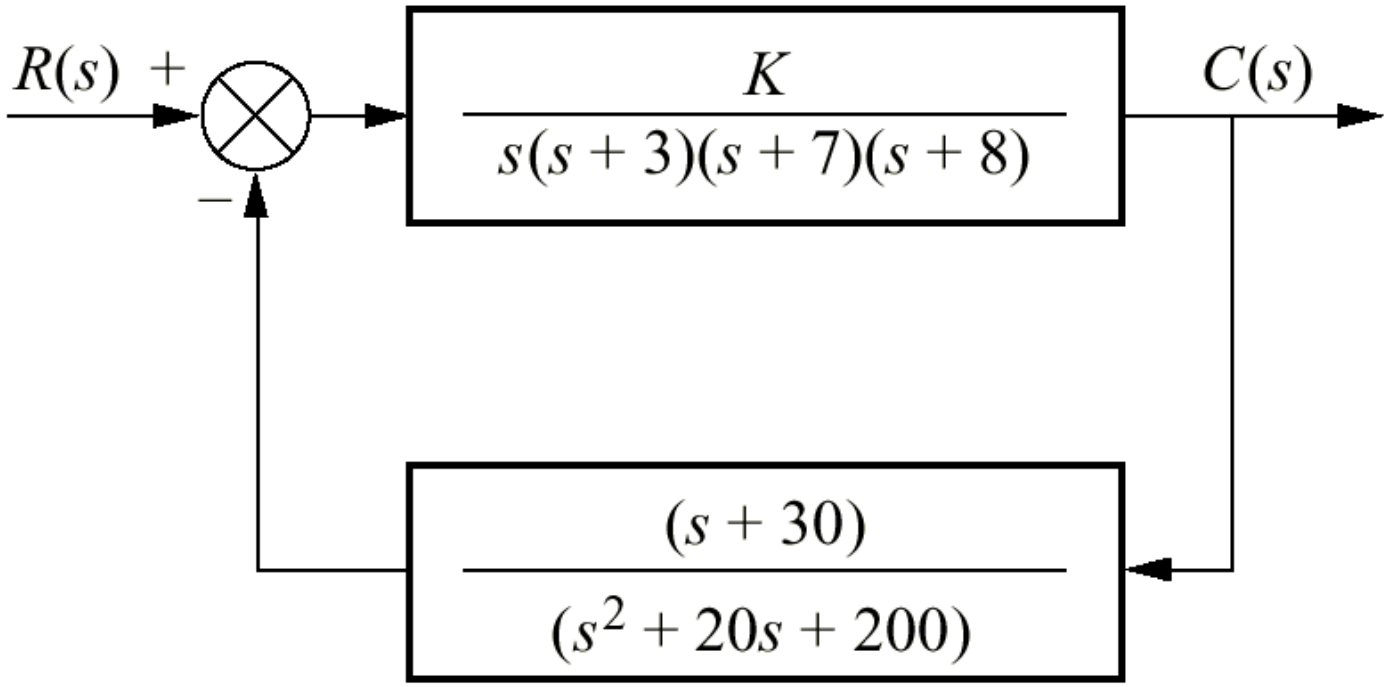

Courtesy of FANUC Robotics.

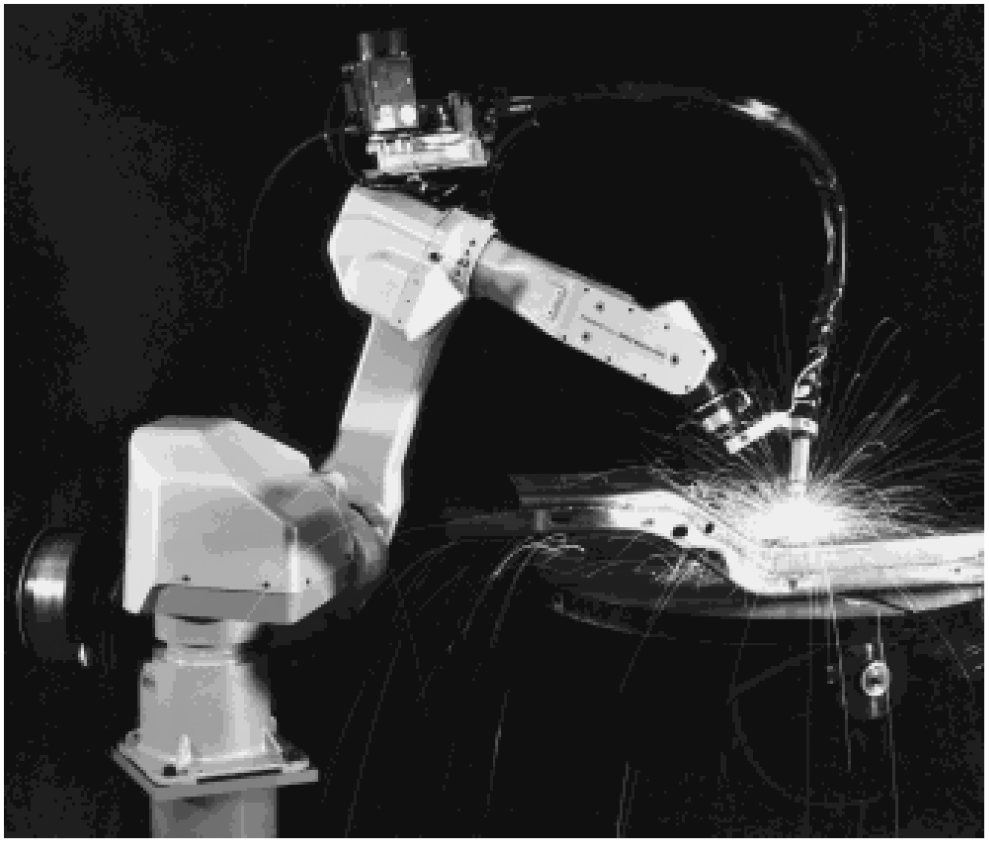

(*a*)

Figure P8.13

a. Robot equipped to perform arc welding;
(*figure continues*)

Figure P8.13
(continued)
b. block diagram for swing motion system

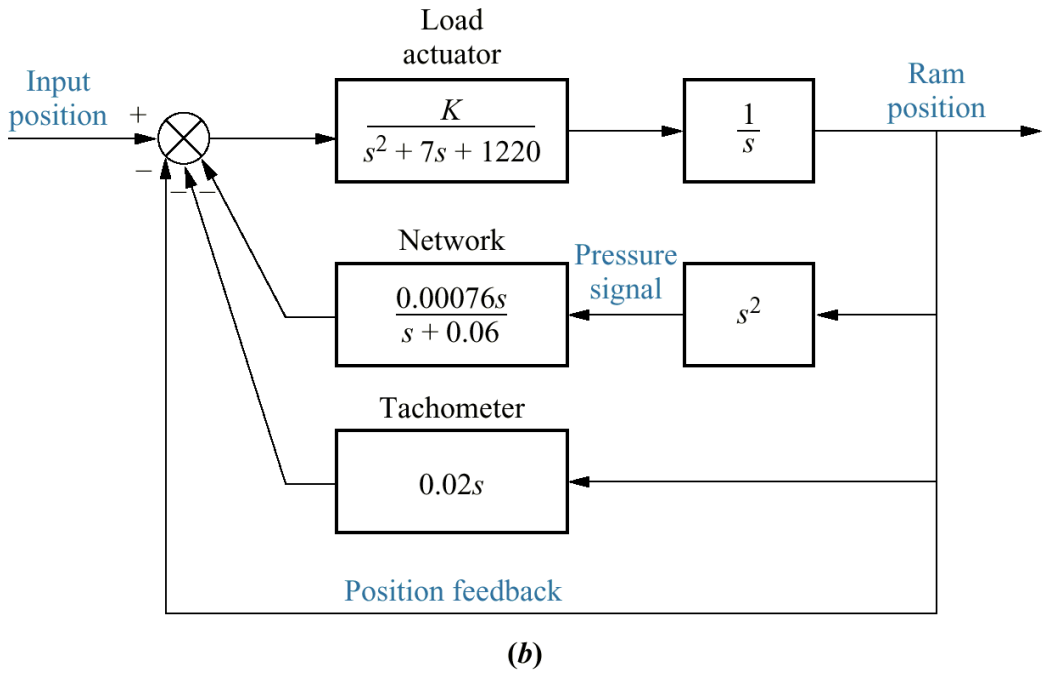

(*b*)

Figure P8.14
Block diagram of smoother

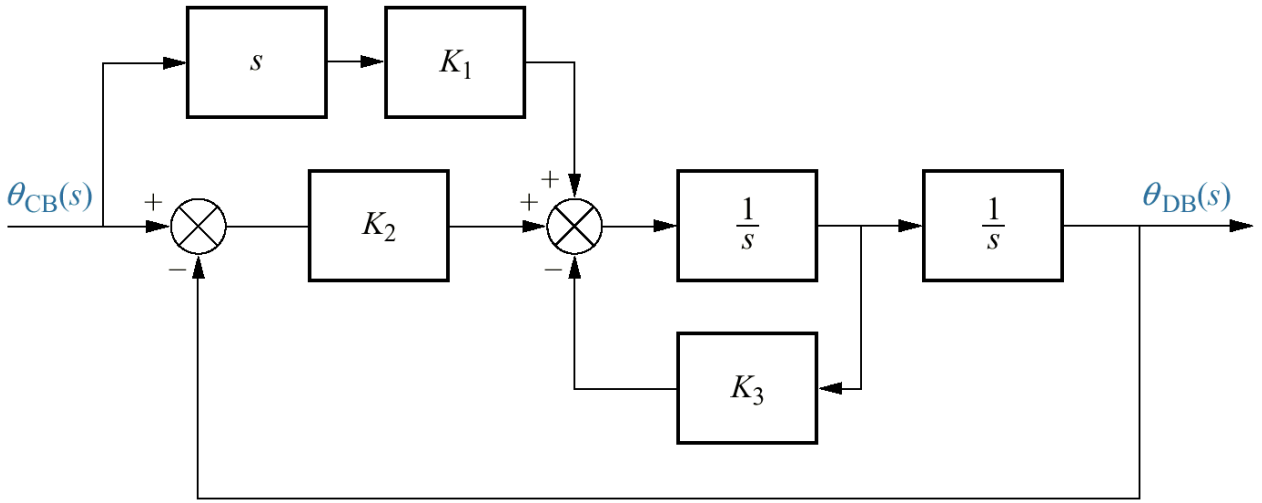

Figure P8.15
a. Active vibration absorber ((c)1992 AIAA);
b. control system block diagram

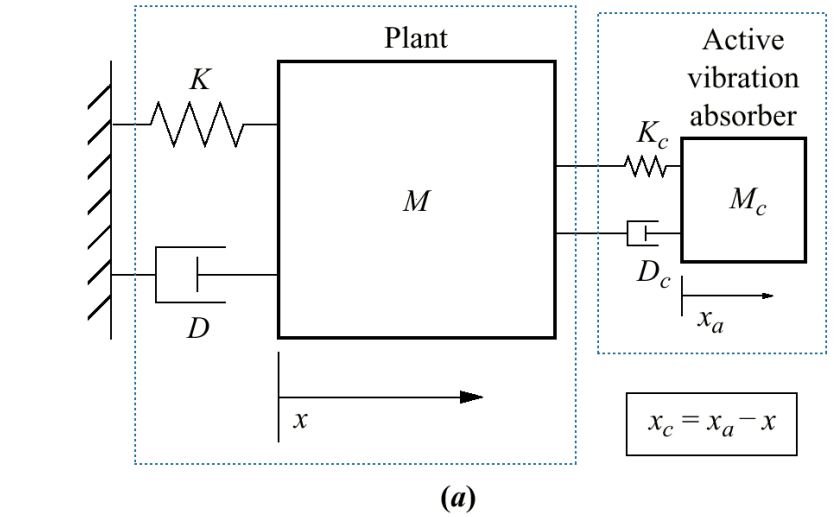

(a)

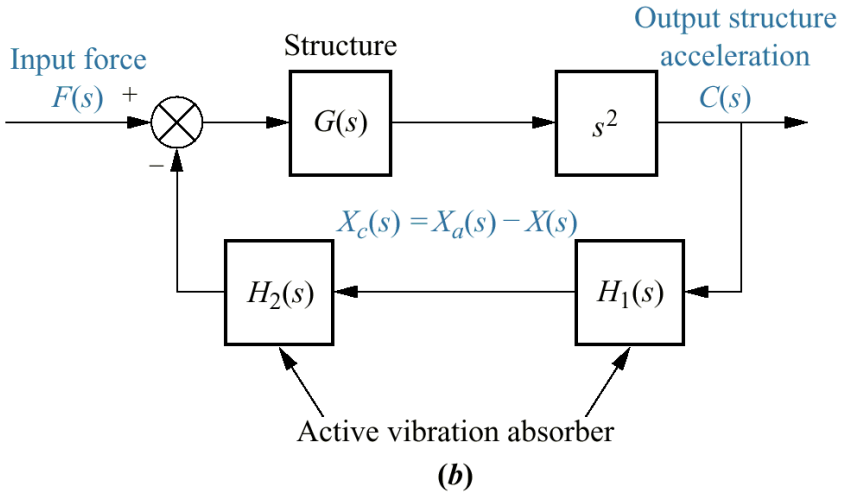

(b)

Figure P8.16
Floppy disk drive:
a. physical representation;
b. block diagram

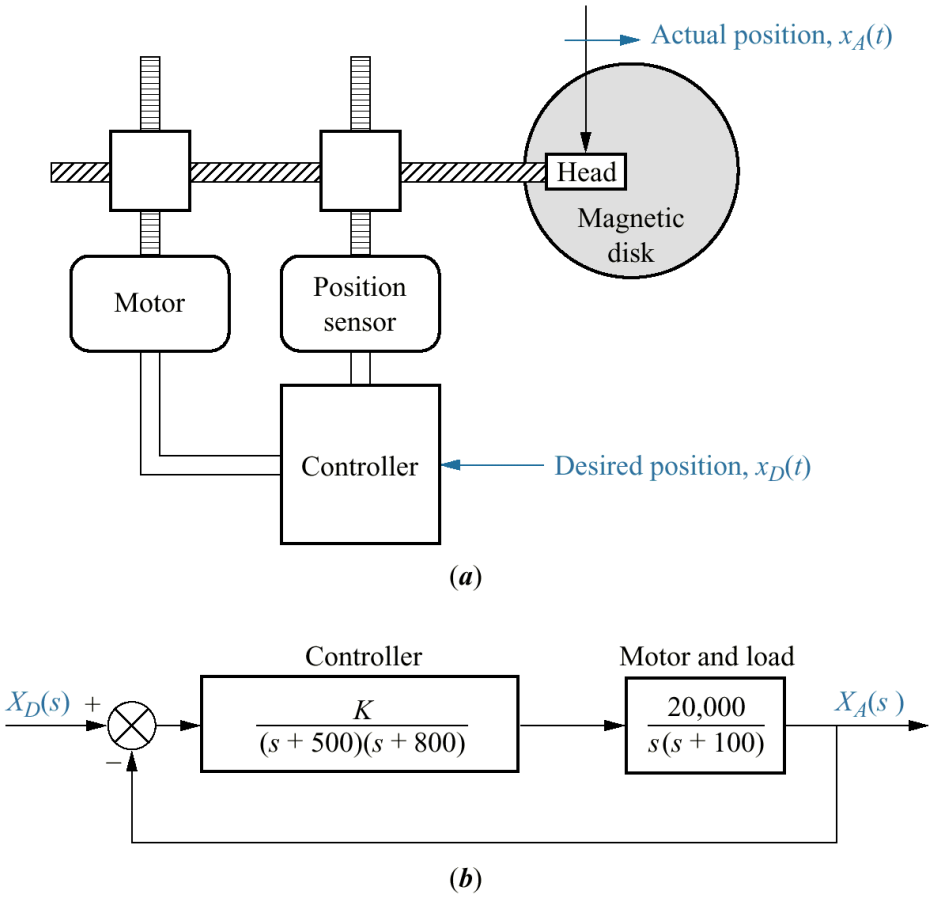

Figure P8.17
Simplified block diagram of pupil servomechanism

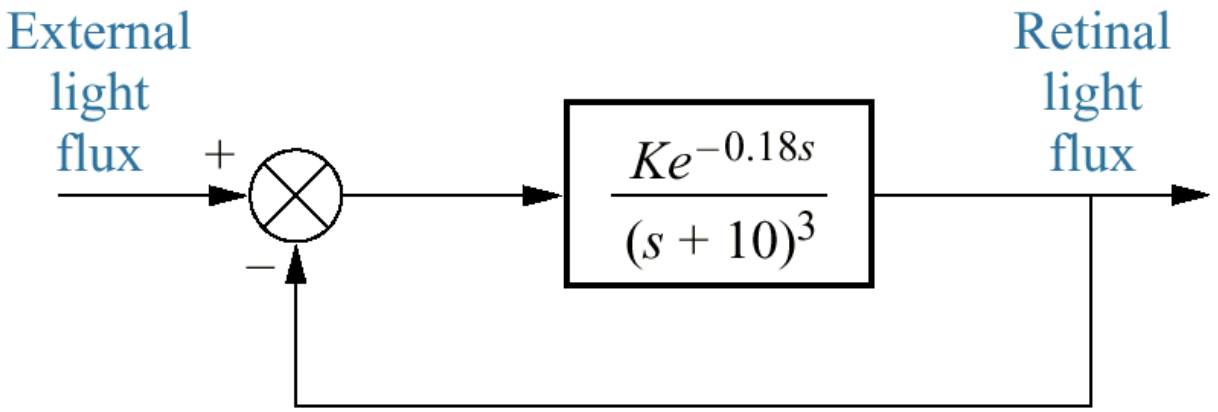

Figure P8.18
Active suspension system

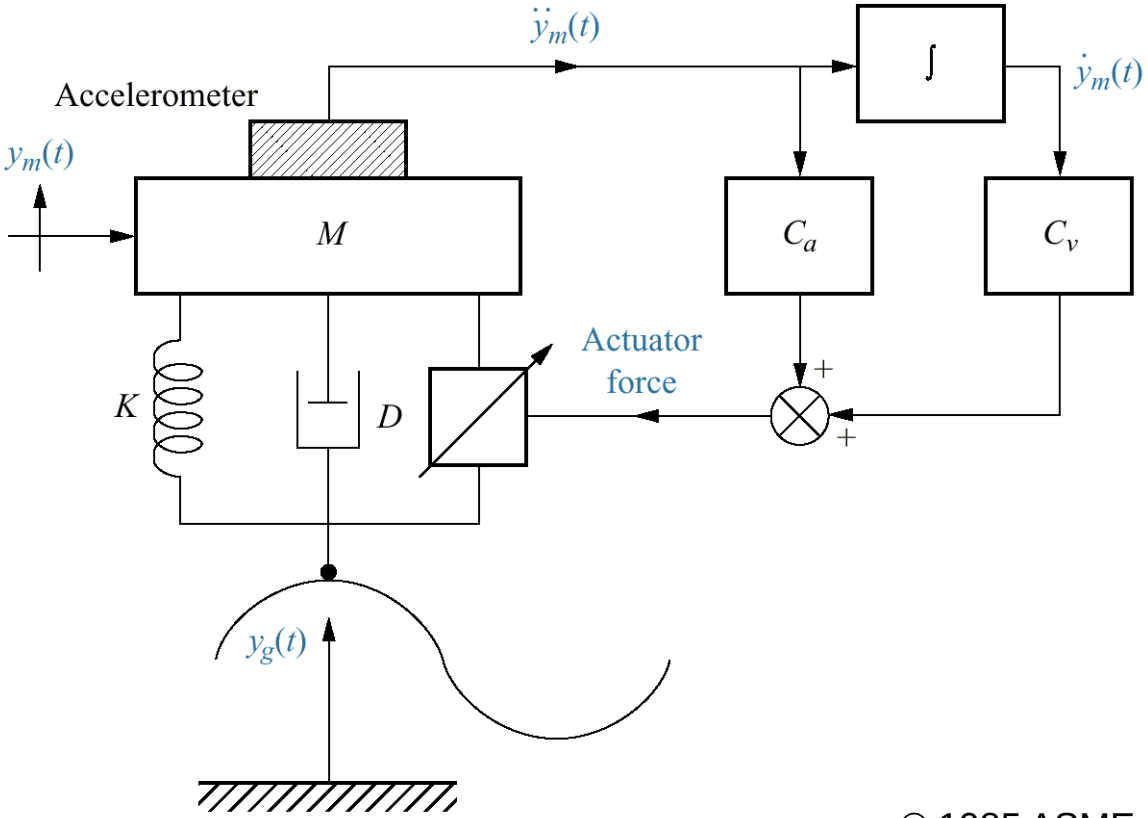

Figure P8.19
F4-E pitch stabilization loop

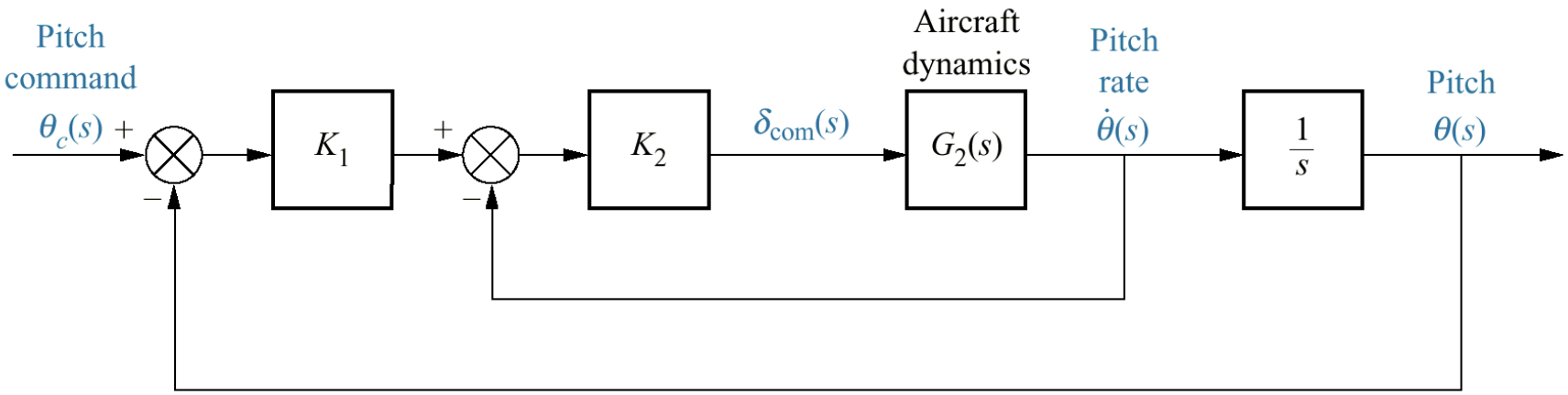

Figure P8.20
Pitch axis attitude control system utilizing momentum wheel

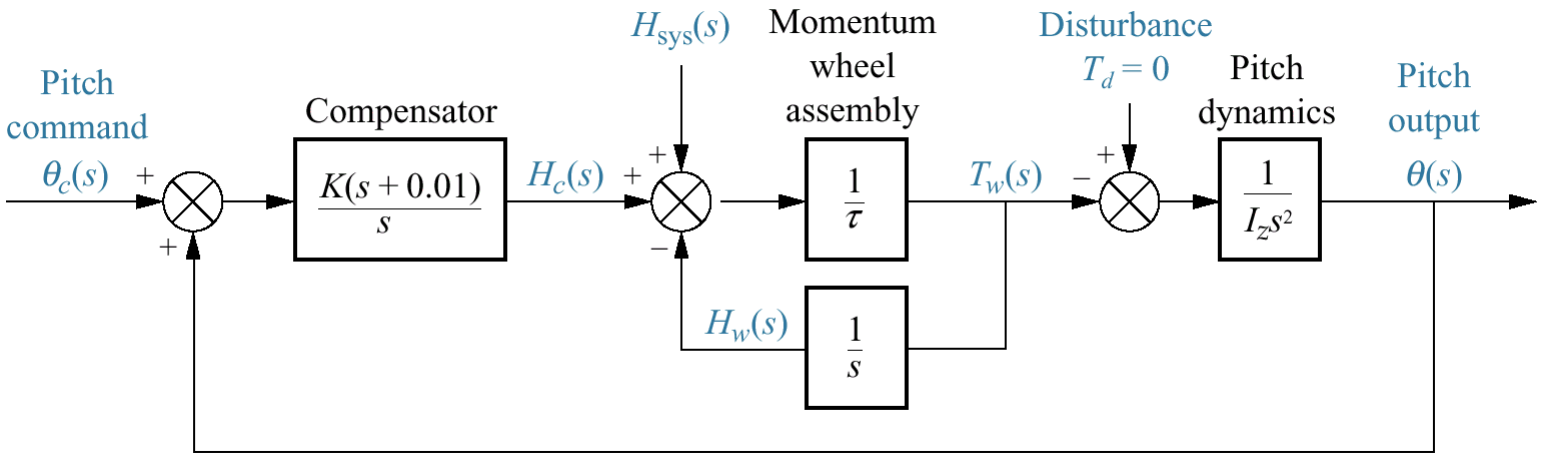

Figure P8.21

a. Combustor with microphone and loud speaker ((c)1995 IEEE);

b. block diagram ((c)1995 IEEE)

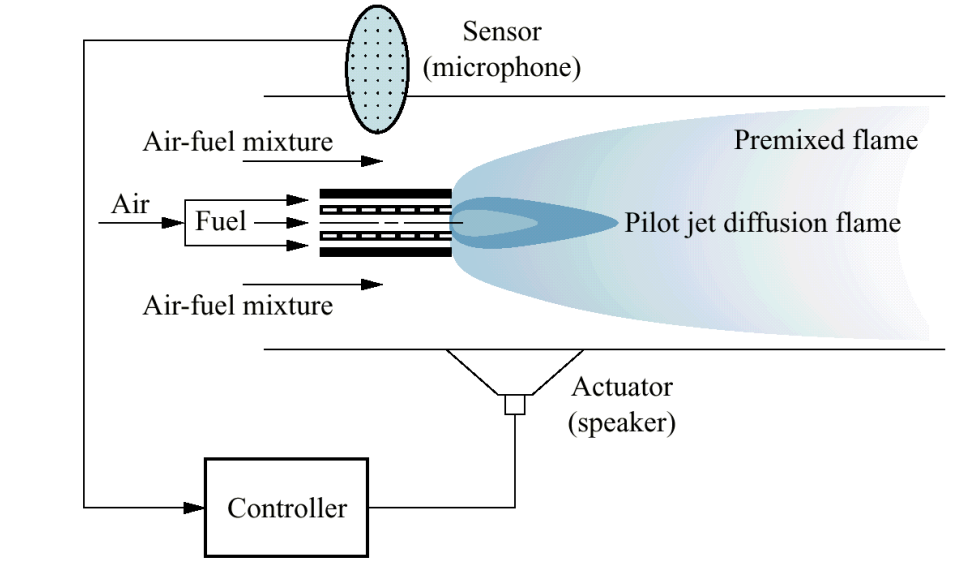

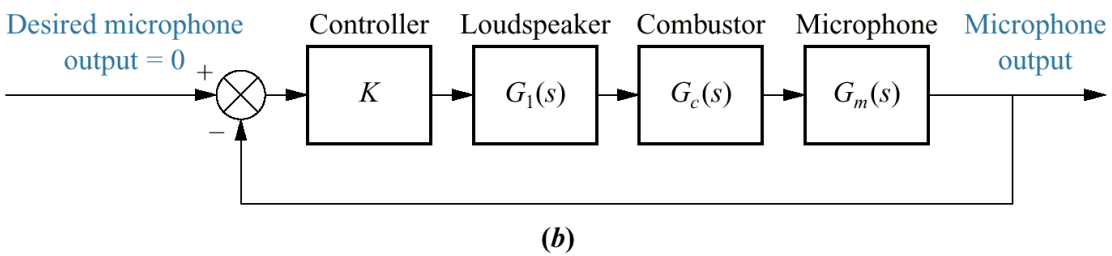

(*a*)

Figure P8.22

a. Wind turbines generating electricity near Palm Springs, California;

(figure continues)

Figure P8.22
(*continued)*
b. Control loop for a constant-speed pitch-controlled wind turbine ((c)1998 IEEE);
c. Drivetrain ((c)1998 IEEE)